ALMA MATER STUDIORUM · UNIVERSITÀ DI BOLOGNA

Scuola di Scienze
Corso di Laurea Magistrale in Fisica del Sistema Terra

Initial Validation of an Agile Coupled Atmosphere-Ocean General Circulation Model

Relatore:
Dr. Paolo Ruggieri

Presentata da:
Carlo Grancini

Correlatori:
Dr. Salvatore Pascale
Dr. Fred Kucharski
Dr. M. Adnan Abid

Sessione III
Anno Accademico 2020/2021

Abstract

Mathematical models based on physics, chemistry and biology principles are one of the main tools to understand climate interactions, variability and sensitivity to forcings. Model performance must be validated checking that results are consistent with actual/observed climate.

This work describes the initial validation of a new intermediate complexity, coupled climate model based on a set of existing atmosphere, ocean and sea-ice models. The model, developed and made available by the International Centre for Theoretical Physics (ICTP), is based on the widely used SPEEDY atmospheric model. However, limited literature is available for its version, coupled to the NEMO ocean model referred to as SPEEDY-NEMO. The focus of this study is on the adaptation and validation of this model.

A long-term spin-up run with constant present-day forcing has been performed to achieve a steady-state climate. The simulated climate has then been compared with observations and reanalyses of the recent past. The initial validation has shown that simulations spanning a thousand years can be easily run. The model does not require many h/w resources and therefore significant size samples can be generated if needed.

Our results prove that long timescale, stable simulations are feasible. The model reproduces the main features of Earth's mean climate and variability, despite the use of a fairly limited resolution grid, simple parameterizations and a limited range of physical processes.

Ocean model outputs have not been assessed. However a clear El Niño signal in the simulated Sea Surface Temperatures (SSTs) data and arctic sea ice extent show that the ocean model behaviour is close to observations.

According to the results the model is a promising tool for climate studies. However, to understand its full potential the validation should be improved and extended with an analysis of ocean variables and targeted simulations with modified conditions to evaluate model behaviour under different conditions.

Sommario

I modelli matematici basati su principi di fisica, chimica e biologia sono uno degli strumenti principali per comprendere la variabilità delle interazioni climatiche e la sensibilità alle forzanti. I risultati del modello devono essere validati per garantire che siano coerenti con il clima effettivo/osservato. La validazione può essere eseguita confrontando le simulazioni climatiche del modello con le osservazioni.

Questo lavoro descrive la convalida iniziale di un nuovo modello climatico accoppiato di complessità intermedia basato su una serie di modelli esistenti di atmosfera, oceano e ghiaccio marino. Il modello, sviluppato e reso disponibile dall'International Center for Theoretical Physics (ICTP), denominato SPEEDY, è stato ampiamente utilizzato nella comunità climatica nella sua sola versione atmosferica. Ad ora è disponibile una letteratura limitata per la versione in cui SPEEDY è accoppiato al modello oceanico NEMO. La versione accoppiata oceano-atmosfera è chiamata SPEEDY-NEMO. In questo studio, l'attenzione si concentra sull'adattamento e sulla convalida di SPEEDY-NEMO, che saranno la base per il lavoro futuro.

Dopo un lungo spin-up con forzanti corrispondenti al periodo attuale per raggiungere un clima stazionario, il clima simulato è stato confrontato con osservazioni e rianalisi del recente passato.

La convalida iniziale ha dimostrato che il modello può essere portato su un nuovo server con uno sforzo limitato e che è possibile eseguire facilmente lunghe simulazioni che coprono migliaia di anni. Il modello richiede risorse h/w limitate e quindi, se necessario, è possibile generare campioni di dimensioni significative.

I risultati dimostrano che sono possibili simulazioni stabili e su tempi lunghi. Il modello riproduce le principali caratteristiche del clima medio terrestre e della sua variabilità, nonostante l'uso di una griglia a risoluzione abbastanza limitata, parametrizzazioni semplici e una gamma limitata di processi fisici.

I risultati del modello oceanico non sono stati valutati. Tuttavia i dati delle temperature superficiali del mare (SST) simulati dal modello, mostrano un chiaro segnale di El Niño e anche il ghiaccio marino artico mostra che il comportamento del modello oceanico è vicino alle osservazioni.

I risultati mostrano che il modello è uno strumento promettente per gli studi sul clima. Tuttavia, per comprendere il suo pieno potenziale, la convalida deve essere migliorata ed estesa con un'analisi delle variabili oceaniche e simulazioni mirate con condizioni modificate per valutare il comportamento del modello in condizioni diverse.

CONTENTS

1. Introduction

The importance of climate - here broadly defined as all of the statistics describing the atmosphere and ocean in a particular region - to human beings is so fundamental that we often overlook it. If the climate was not more or less as it is now, civilizations and life on Earth would have not thrived as they have. Climate affects human lives in many ways; for example, it influences the type of housing people have developed, or the kind of agricultural procedures people can use in different parts of the world to produce food.

In our contemporary world, with the huge technological advances of the past century, one might think that climate is no longer a force capable of changing the destiny of human history. On the contrary, a close analysis of the problem reveals that the contemporary world, with billions of people mostly concentrated in large cities and who heavily rely on technology and advanced food production systems, is as sensitive now as we have ever been to climate fluctuations and climatic change.

Since energy, water and food supply systems are optimized to the current climate, fluctuations and shifts in climate can indeed cause serious problems for humanity. Furthermore, as the world population has grown to absorb the maximum agricultural productivity, the number of people at risk of starvation during climatic anomalies has never been higher. Therefore, there are serious concerns about the role of human activities in causing long-term changes in the climate. As reaffirmed once more by the sixth IPCC Assessment Report on the state of the climate (Masson-Delmotte, et al., 2021), it is now unequivocable that humans are warming the global climate by altering the composition of the atmosphere – by emitting greenhouse gases, mostly carbon dioxide and methane, as a result of fossil fuels combustion, and aerosols deriving from industrial and agricultural activities - and the nature of the Earth's surface, and this influence is becoming increasingly larger.

1.1. The Climate System

The climate system is composed of the atmosphere, hydrosphere, cryosphere, land surface and biosphere, and their interactions.

Figure 1 (IPCC, 2001) shows a schematic view of the climate system components.

The *atmosphere* is the most unstable and rapidly changing part of the system. Its composition (78.1% nitrogen, 20.9 % oxygen, 0.83% Argon, etc.), which has changed with the evolution of the Earth, is of central importance to the problem of anthropogenic climate change. In particular, the so called greenhouse gases (carbon dioxide, methane, nitrous oxide, etc., while occupying less than 0.1% by volume, play an essential role in the Earth's energy budget.

The *hydrosphere* is the component comprising all liquid water, that is rivers, lakes and aquifers, oceans and seas. The oceans cover approximately 70% of the Earth's surface. Oceans store and transport a large amount of energy and dissolve and store great quantities of carbon dioxide. Mainly

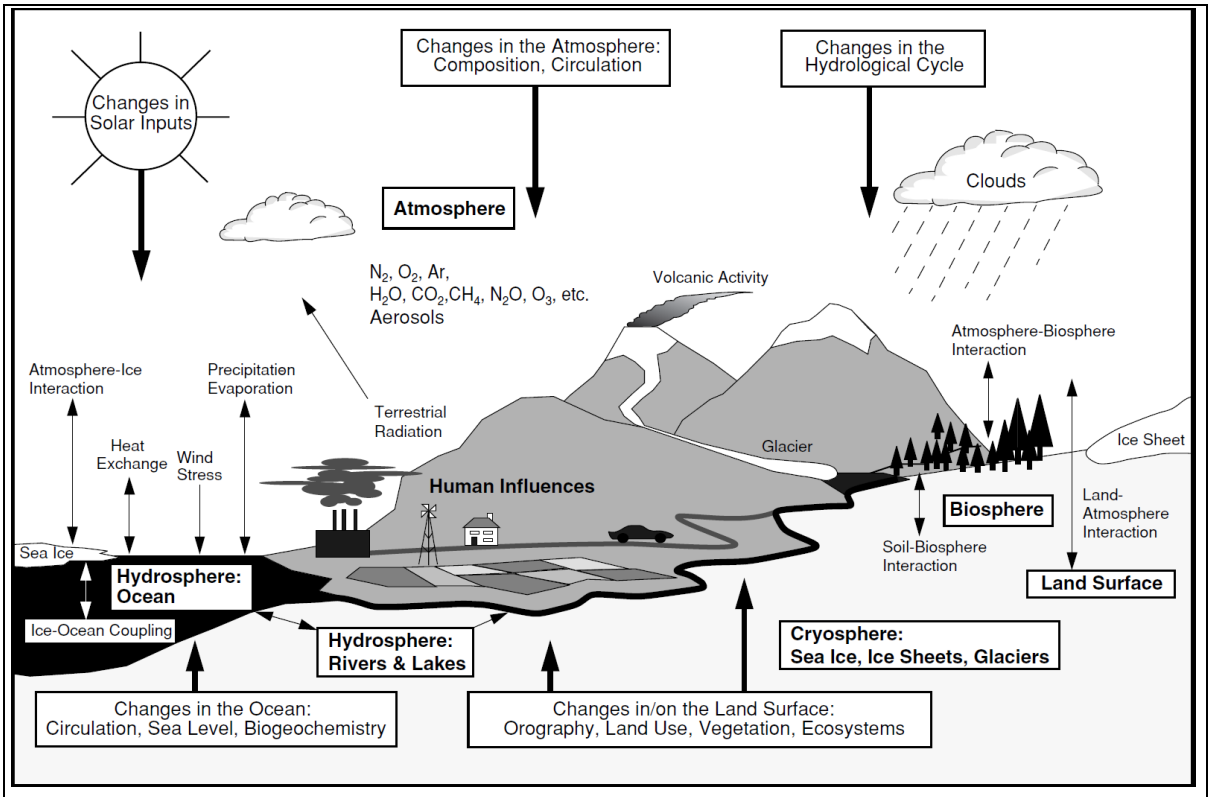

Figure 1 Climate system components from (IPCC, 2001)

due to the large thermal inertia of the oceans, they damp vast and strong temperature changes and function as a regulator of the Earth's climate and as a source of natural climate variability, in particular on the longer timescales.

The *cryosphere*, including the ice sheets of Greenland and Antarctica, continental glaciers and snow fields, sea ice and permafrost, has a key role within the climate system because of its high reflectivity (albedo) for solar radiation and its critical role in driving deep ocean water circulation. Because the ice sheets store a large amount of water, variations in their volume are a potential source of sea level variations.

Vegetation and soils at the *land surface* control how energy received from the Sun is returned to the atmosphere. Some is returned as long-wave (infrared) radiation, heating the atmosphere as the land surface warms. Some serves to evaporate water, either in the soil or in the leaves of plants, bringing water back into the atmosphere.

The marine and terrestrial *biospheres* have a major impact on the atmosphere's composition. The biota influences the uptake and release of greenhouse gases. Through the photosynthetic process, both marine and terrestrial plants (especially forests) store significant amounts of carbon from carbon dioxide. Thus, the biosphere plays a central role in the carbon cycle, as well as in the budgets of many other gases, such as methane and nitrous oxide.

Many physical, chemical and biological processes occur among the various components of the climate system on a wide range of space and time scales. This makes the system extremely complex. Components of the climate system are all linked by fluxes of mass, heat and momentum: as a result, all subsystems are open and interrelated amongst them. As an example, the oceans and the atmosphere are strongly coupled and exchange water vapour and heat through evaporation. This is part of the water cycle and leads to condensation, cloud formation, and precipitation in the atmosphere. Precipitation has also an influence on salinity, which on turn influences seawater density and so ocean circulation.

1.2. Modelling the Climate

To understand and predict climate and its variations we need to incorporate the principles of physics, chemistry and biology into a mathematical model of climate, which is what we call a *climate model.* Climate models are fundamental tools in climate science as they allow us to understand climate interactions and assess effects of forcings modifications.

Given the size and the complexity of the climate system, there is no single perfect model that can address all questions, so we use models with different level of complexity depending on the problem we want to investigate. The complexity of a climate model can vary enormously, from a simple energy balance model whose solution can be worked out on the back of an envelope, to the very complex, state-of-the-art global climate models (GCMs).

In general, the key component to be considered in building and understanding a climate model are: 1) radiation; 2) dynamics; 3) surface processes; 4) chemistry; 5) resolution in both time and space (Mcguffie & Henderson-Sellers, 2014) The relative importance of these processes can be visualized using the climate modelling pyramid (Figure 2). The edges of the pyramid represent the basic elements of the model, while complexity increases upwards. Therefore, the simpler models, which have only one primary process, are around the base of the pyramid. There are basically four types of models:

1. Energy balance models (EBMs): zero- or one-dimensional models predicting the surface temperature as a function of the energy balance of the Earth.
2. One-dimensional models: typically radiative-convective models single-column models which focuses on processes in the vertical.
3. Dimensionally constrained models: these models take a wide variety of forms, from the statistical dynamical models to Earth System Models of Intermediate Complexity (EMICs)
4. Global circulation models (GCMs): they account for the three-dimensional nature of the atmosphere and ocean and so they are the types of models that can produce the most realistic simulations of climate.

In the following, our discussion will focus solely on the GCMs. GCMs are often also called “comprehensive” climate models as they incorporate many different processes (Figure 3). Because of the large number of equations to be solved, they generally require the fastest and biggest

computers presently available. GCMs are generally used for two purposes: 1) understanding the climate system and how the various processes interact in present and changing climate conditions;

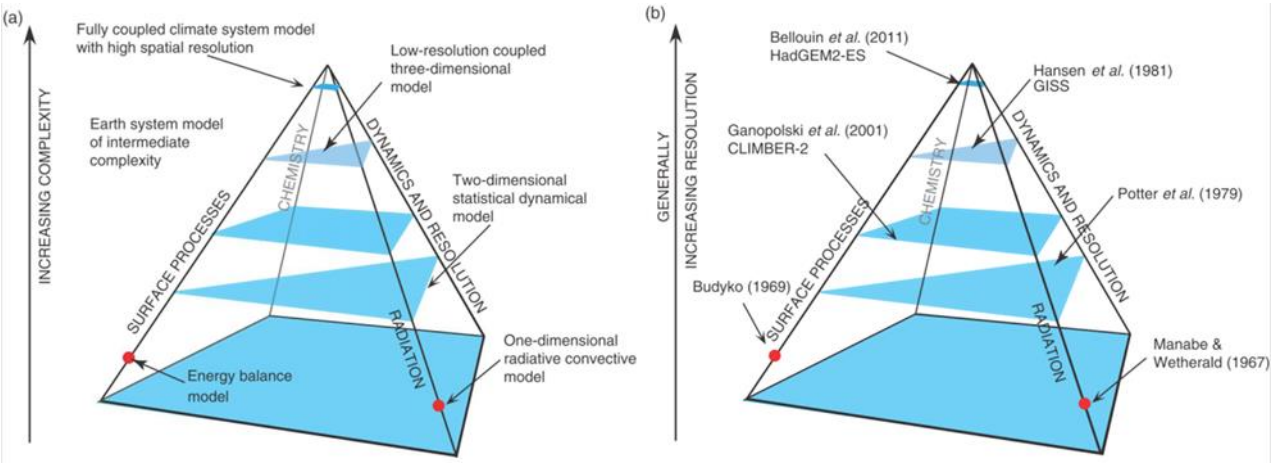

Figure 2 The climate modelling pyramid. The position of a model on the pyramid indicates the complexity with which the four primary processes interact. Progression up the pyramid leads to greater interaction between each primary process. (a) The position of various model types; (b) Examples from the literature and their position on the pyramid. Adapted from (Mcguffie & Henderson-Sellers, 2014)

2) as tools to predict future climates with sufficient details in order to be useful for future planning, as done, for example, in the latest IPCC assessment report on the present climate and for future climate projections (Masson-Delmotte, et al., 2021). The latest development for comprehensive climate models is Earth System Models, which include also the carbon cycle, soil evolution, dynamic vegetation, and biological models. (Claussen, et al., 2002)

Within the category of the GCMs, a hierarchy of progressively less complex climate models exists. These models, which offer less detail, are useful to gain understanding of the key climatic processes and are referred to as *Intermediate-complexity* GCMs (Molteni, Atmospheric simulations using a GCM with simplified physical parametrizations. I. Model climatology and variability in multi-decadal experiments., 2003) (Fraedrich, Jansen, Kirk, Luksch, & Lunkeit, 2005) (Petoukhov, et al., 2000) (Platov, Krupchatnikov, Martynova, Borovko, & Golubeva, 2017) (Kucharski F. , et al., 2013) In fact, we typically gain some understanding of a complex system by relating its behaviour to that of simpler systems. For sufficiently complex systems, we thus need a model hierarchy on which to base our understanding, describing how the dynamics change as key sources of complexity are added or subtracted (Held I. , 2005) GCMs with intermediate representation of physical processes thus

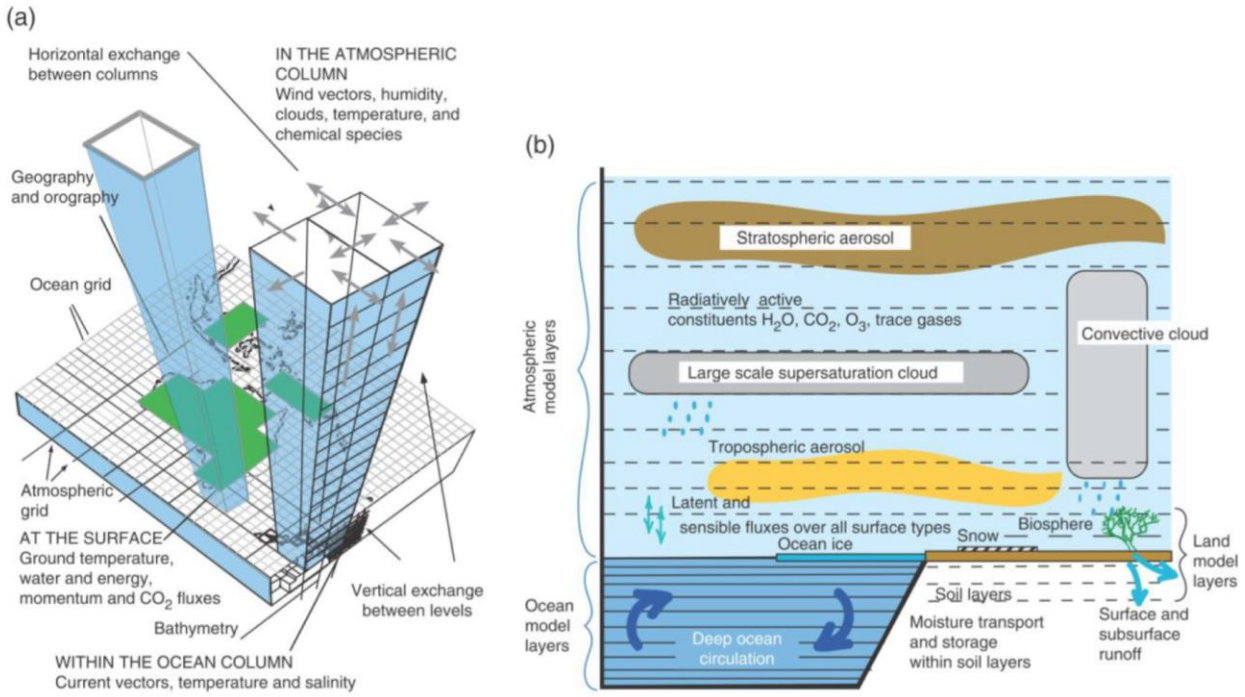

Figure 3 Illustration of the basic features of a global climate model. (a) Discretization is a basic characteristic of three-dimensional climate models. Both the atmosphere and ocean are modelled as a set of interacting columns distributed across the Earth's surface. The resolution of the atmosphere and the ocean are usually different. (b) Schematic illustration of the processes in a single column of a GCM, including various types of clouds, soil layers and aerosols. Adapted from (Mcguffie & Henderson-Sellers, 2014)

represent a class in the hierarchy of models between the simpler, idealized models and the comprehensive state-of-the art GCMs.

Intermediate-complexity GCMs describe the dynamics of the atmosphere and/or ocean in a way which is less detailed than state-of-the-art GCMs but, at the same time, much more realistic and complex than in EBMs or ocean box models. As their more sophisticated siblings, Intermediate complexity GCMs use parameterizations of the unresolved flow or explicitly resolve the equations of geophysical fluid dynamics, even though parametrizations are less sophisticated, and dynamical cores are at a coarser spatial resolution, than what used in state-of-the-art GCMs.

Intermediate complexity models reduce detail to allow for the simulation of more processes and longer time spans and therefore have an important place in the model range.

As they run fast, intermediate-complexity GCMs can be used to simulate millennia and longer timespans with relatively short computer time or generate large ensembles of simulations to differentiate the forced signal from that of internal climate variability. Moreover, they can use

inexpensive hardware like workstations and thus can be used also by institutions that do not have the financial resourced to buy time on mainframes or expensive computational resources.

Another important area where intermediate complexity models are widely used is in the work of graduate students, who gain better scientific and software insights from a simpler model than those they could get from state-of-the-art GCMs. Some more advantages of intermediate complexity models are that many of them are well documented and freely available for download and use. They are constructed in a way to facilitate the experimentation with different forcings, coupling approaches, parameterizations, etc., which encourages creativity in pursuing an understanding of the fundamental science (Kucharski et al., 2013).

Finally, intermediate complexity models physical parametrizations can usually be easily modified to investigate effects of changes in the environment, to assess possible evolutions, to evaluate consequences of foreseen or planned changes in climate forcings and to investigate specific interactions.

1.3. SPEEDY-NEMO: a GCM of Intermediate Complexity

An example of an intermediate complexity model is the atmospheric general circulation model (AGCM) developed at the Abdus Salam International Centre for Theoretical Physics—the ICTPAGCM, also called SPEEDY, from Simplified Parameterizations, primitivE-Equation DYnamics (Molteni, 2003) (Kucharski F. , et al., 2013). The ICTPAGCM model is very flexible in the sense that it can be easily modified to address a wide range of problems. While there is wide documentation about the SPEEDY model and its use is documented in a number of studies (e.g., (Molteni, King, Kucharski, & Straus, 2010) (Kucharski, Molteni, & Bracco, 2006); (Kucharski, Zeng, & Kalnay, 2012); (Barimalala, Bracco, & Kucharski, 2011); (Feudale & Kucharski, 2013), less documented is a more recent development of this model which includes coupling of SPEEDY to a dynamical ocean model, the Nucleus for European Modelling of the Ocean (Madec, et al., 2013). The SPEEDY-NEMO configuration has been used in several studies (e.g., (Kucharski, et al., 2015) (Sluka, Penny, Kalnay, & Miyoshi, 2016))but there is not a systematic validation of it. This will be the goal of the present work.

2. The SPEEDY-NEMO Atmosphere-Ocean General Circulation Model

In this chapter we provide a detailed description of the SPEEDY-NEMO coupled atmosphere-ocean general circulation model. We will give details about the atmospheric model component, the ocean model component and the coupling between the two through the OASIS coupler. The model has been developed at ICTP (ICTP - International Centre for Theoretical Physics, s.d.) with the aim of understanding the global climate interactions at different time scales. The "ICTP AGCM" also known as SPEEDY has been adapted and coupled to the NEMO ("Nucleus for European Modelling of the Ocean") ocean model which includes LIM, the Louvain-la-neuve sea Ice Model. SPEEDY has proved quite flexible in relatively large ensemble simulations (Ehsan, Kang, Almazroui, Abid, & Kucharski, 2013) (Abid, Kang, Almazroui, & Kucharski, 2015) and SPEEDY-NEMO will be certainly useful for the same class of applications.

Coupling of the ocean and atmosphere models is performed by means of the OASIS3 coupler. As detailed below the atmosphere model has a spatial resolution of about 3,75° x 3,75° (spectral truncation T30) and NEMO of half a degree at the equator and 2° at most other latitudes. Considering the Rossby radius of deformation the relative resolution of the atmosphere model is better than the resolution of the ocean model.

2.1. Atmosphere Model

2.1.1. Dynamic core

The atmosphere is modelled by SPEEDY ("Simplified Parameterizations, privitivE-Equation DYnamics") AGCM (Molteni, 2003) (Kucharski, Molteni, & Bracco, 2006) (Kucharski F. , et al., 2013). The model is based on hydrostatic spectral dynamical core originally developed at the Geophysical Fluid Dynamics Laboratory (Held & Suarez, 1994). Core model is described in detail in (Bourke,

1974). A detailed description can also be found on the ICTP web site (Kucharski F. , Speedy ver 41 Description)

The core solves the fluid dynamics equations:

$$\frac{d\vec{v}}{dt} = -f\vec{k} \times \vec{v} - \vec{\nabla}\Phi - RT\vec{\nabla}p_s + \vec{F}$$ Horizontal momentum

$$\frac{dT}{dt} = \frac{RT}{c_p}\left(\frac{\dot{\sigma}}{\sigma} - \frac{\partial\dot{\sigma}}{\partial\sigma} - \vec{\nabla}\cdot\vec{v}\right) + \frac{Q}{c_p}$$ Conservation of energy

$$\frac{d\ln p_s}{dt} = -\vec{\nabla}\cdot\vec{v} - \frac{\partial\dot{\sigma}}{\partial\sigma}$$ Continuity equation

$$\frac{d\Phi}{d\sigma} = -\frac{RT}{\sigma}$$ Hydrostatic approximation

The vertical coordinate is expressed as ratio between pressure and surface pressure (Phillips, 1957):

$$\sigma = \frac{p}{p_0}$$

Moisture variations are described by the following equation where S includes diffusion, phase changes and evaporation at surface.

$$\frac{dq}{dt} = S$$

$\vec{v}$ is replaced by vorticity and divergence

$$\xi = \vec{k}\cdot\vec{\nabla}\times\vec{v}$$

$$D = \vec{\nabla}\cdot\vec{v}$$

the streamfunction and the velocity potential

$$\xi = \nabla^2\psi, \quad D = \nabla^2\chi$$

are used to solve the equations in spectral space.

The model has 8 layers with boundaries at 0, 0.05, 0.14, 0.26, 0.42, 0.60, 0.77, 0.90 and 1 σ (half levels). The 8 full levels are at 0.025, 0.095, 0.20, 0.34, 0.51, 0.685, 0.835 and 0.95 σ. The top two

layers model the stratosphere, while the bottom layer models the boundary layer. Output data are post-processed on pressure levels at 30, 100, 200, 300, 500, 700, 850 and 925 hPa

Gravity waves are treated semi-implicitly. Leapfrog integration with an additional Robert filter (Robert, 1966) is performed.

A triangular spectral truncation at 30 (T30) is applied. A gaussian grid of 96 by 48 provides a resolution of about 3.75° at the equator (about 400 km). The grid is rectangular and has no points at the poles (see Figure 12 bottom)

Spectral quantities are converted to geometrical ones and back at each timestep to perform computations of physical quantities and parametrizations.

2.1.2. Physical parametrizations

A set of simplified physical parametrization schemes has been developed based on principles used in more complex models, with several simplifying assumptions which are suited to a model with a coarse vertical resolution. These parameterizations are:

Convection

A simplified mass-flux scheme is activated in unstable regions, and where humidity in the planetary boundary layer (PBL) exceeds a certain threshold. The cloud-base mass flux is such that the PBL humidity is relaxed towards the threshold value on a time-scale of 6 hours. Detrainment occurs only at the cloud- top level, whereas entrainment occurs in the lower half of the troposphere. The air in the updrafts is assumed to be saturated.

Large-scale condensation

Where relative humidity exceeds a threshold, specific humidity is relaxed towards the corresponding threshold value on a time-scale of 4 hours, and the latent heat content removed from the atmosphere is converted into dry static energy.

Clouds

Cloud cover and thickness are derived diagnostically from the values of relative humidity in an air column including all tropospheric layers except the PBL and the amount of total precipitation. Stratocumulus clouds are treated separately based on the static stability in the PBL.

Short-wave radiation

The shortwave radiation schemes use two spectral bands, one of which represents the near-infrared portion of the spectrum. Radiation is reflected at cloud top and at the surface; the cloud albedo is proportional to the total cloud cover. The shortwave transmissivities of the model layers are functions of layer mass, specific humidity and cloud cover.

Long-wave radiation

The longwave radiation schemes use four spectral bands, one for the atmospheric ”window” and the other ones for the spectral regions of absorption by water vapour and carbon dioxide. For each layer, transmissivities in the four bands are defined as a function of layer mass and humidity. The effect of clouds is represented as a decrease in the transmissivity of the ”window” band, as a function of cloud cover.

Surface fluxes of momentum and energy

Surface fluxes are derived bulk aerodynamic formulas with different exchange coefficients between land and sea. Coefficients for heat fluxes also depend on a simple stability index, while the coefficient for the momentum flux over land is a function of topographic height. A skin temperature over land is defined from the surface energy balance.

Vertical diffusion

Vertical diffusion is composed of three terms: a redistribution of dry static energy and moisture between the two lowest model layers, which simulates shallow convection in regions of conditional instability; a diffusion of water vapour in stable conditions which acts in the lower troposphere, depending on the vertical profile of relative humidity; and a diffusion of dry static energy in case the lapse rate approaches the dry-adiabatic limit.

For a more detailed mathematical description of the parameterizations see (Kucharski F. , Speedy ver 41 Description)

2.2. Ocean Model

The oceans are modelled by NEMO: Nucleus for European Modelling of the Ocean (NEMO ocean model, s.d.). NEMO is composed of several modules. The main ones are OPA and LIM. SPEEDY-NEMO uses version 3.0 of NEMO.

2.2.1. Fluid Dynamics Equations Solver: OPA

OPA ("Océan PArallélisé") solves the primitive fluid dynamics equations (Madec & Delecluse, Ocean General Circulation Model Reference Manual). A nonlinear equation of state $\rho = \rho(T, S, p)$ is added to the fluid dynamics equations to link temperature and salinity, the two active tracers, to the fluid velocity. The Jackett and McDougall formulation of the equation of state (Jackett & Mcdougall, 1995) has been used to improve performance. The model, in addition, assumes the following:

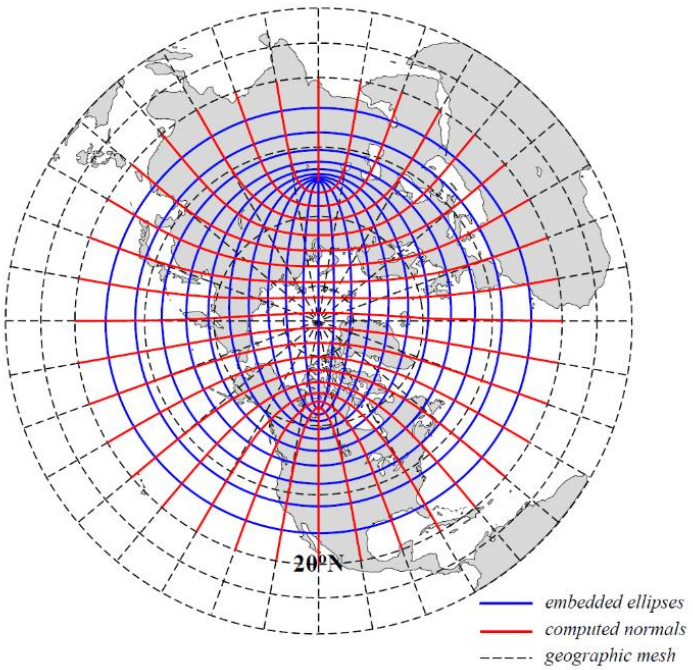

Figure 4 ORCA2 north pole grid from (Madec, et al., 2013)

The geopotential surfaces are spheres. Gravity is parallel to the Earth's radius. The ocean depth is negligible with respect to Earth radius The turbulent fluxes (which represent the effect of small-scale processes on the large-scale) are parametrized from large scale values. Boussinesq approximation is used (density is constant except in connection with gravity) The vertical momentum equation is reduced to the hydrostatic balance. convective processes are therefore parametrized. The three-dimensional divergence of the velocity vector is assumed to be zero which implies incompressibility.

The model uses an ORCA2 tripolar grid which has two poles on land in the northern hemisphere to prevent singularities in the ocean (Figure 4)

The horizontal resolution is 2° reduced to 0,5° around the equator to provide more detail.

The resolution is also increased in the Mediterranean, Red, Black and Caspian Seas. See Figure 5

The z coordinate system has 31 levels. The levels are close to each other near the surface to accurately model the mixed layer and the interaction with the atmosphere.

The numerical solution uses a leapfrog scheme on a staggered Arakawa type C grid (Mesinger & Arakawa, 1976).

The ocean model is run with a time step of 5760 s (which converts to 96 min, or 15 time steps per day) and coupled to the ice model every five time steps.

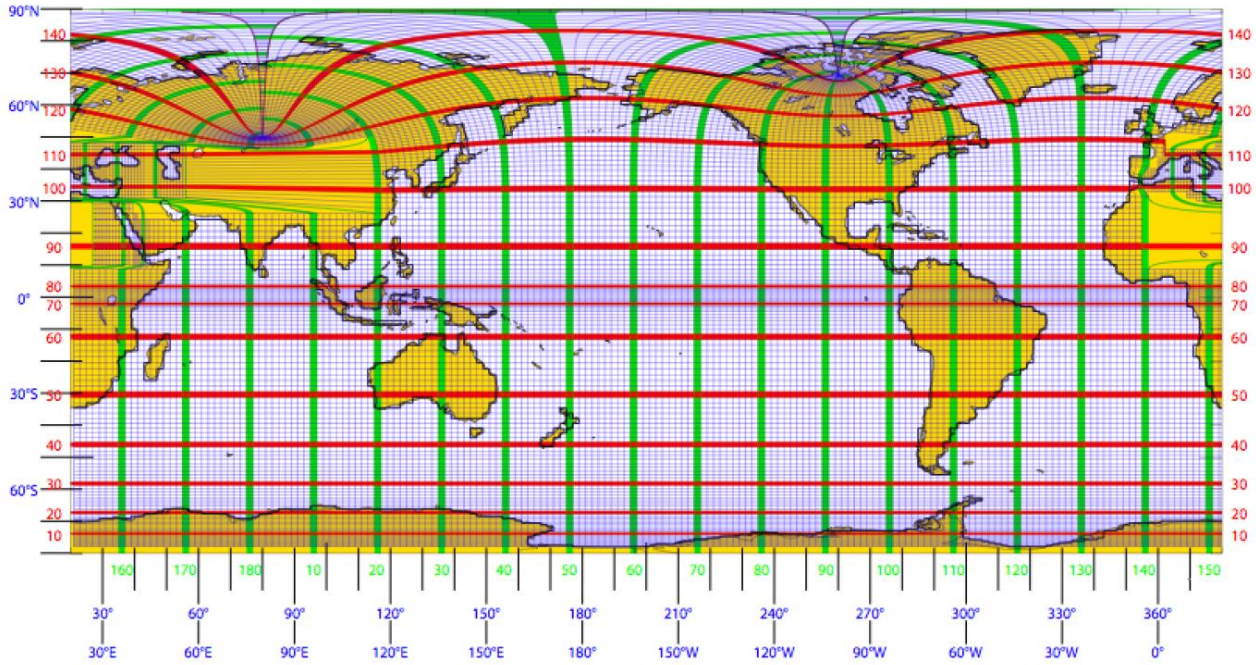

Figure 5 ORCA2 grid. From (Lemaire, 2010) showing the two northern hemisphere "poles" and the increased resolution at the equator and in the Red, Mediterranean, Black and Caspian seas.

The model runs in parallel on the selected number of processors. The earth is divided into domains and a processor is allocated to each domain, see Figure 8.

2.2.2. Louvain-la-Neuve Sea Ice Model

The Louvain-la-Neuve sea ice model (LIM) is a dynamic–thermodynamic model developed for climate studies (Timmermann, et al., On the representation of high latitude processes in the ORCA-LIM global coupled sea ice–ocean model, 2005), (Fichefet & Morales Maqueda, 1997).

The model defines a snow layer and two ice layers for sensible heat storage and vertical heat conduction within snow and ice. Energy budgets at the upper and lower surfaces, and lead surfaces drive vertical and lateral sea ice change rates. The sub grid snow and ice thickness distributions are parametrized by means of an effective thermal conductivity. Storage of latent heat inside the ice resulting from the trapping of shortwave radiation is modelled and surface albedo is parameterized considering cloud cover, whether the surface is frozen or melting and the thickness of the snow and ice covers. High snow load can lead to the formation of a snow ice cap. The ice velocity field is computed from the dynamical interaction with atmosphere and ocean. The main ice variables are advected with the ice drift velocity. Internal stress for different states of deformation is computed. Ice strength is modelled as a function of thickness and concentration. Ice strength parameter has

been set with sensitivity experiments. The formation of leads is parametrized as a function of shearing deformation and small-scale fluctuations of sea ice drift.

Momentum exchange at the ice–ocean interface is computed from the difference between the top layer ocean velocity and ice velocity. Heat flux is assumed to be proportional to the difference between the surface temperature and the temperature at the freezing point and the friction velocity at the ice–ocean interface.

Fresh water fluxes are computed with constant salinities of 6 psu for sea ice and 0 psu for snow.

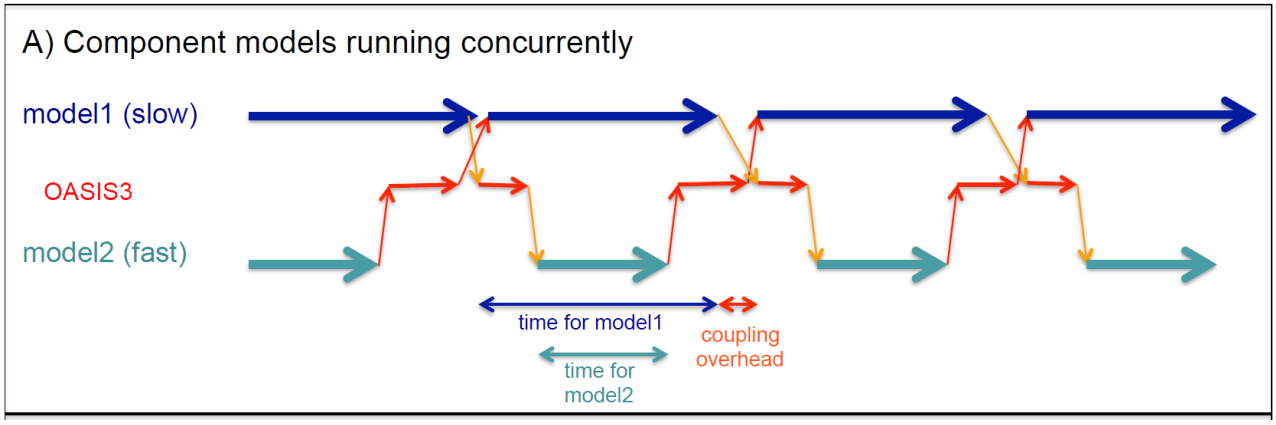

Figure 6 OASIS3 handling of model data exchange. From (Valcke, 2013). SPEEDY NEMO ocean model is slower than the atmospheric model. NEMO in our case would be model1 while SPEEDY would be model2. The diagram represents well the interaction between models, even though it was conceived to show that OASIS3 overhead is limited since it uses the time difference between models to perform its own processing.

2.3. OASIS3 Coupler

The Atmosphere and the ocean models exchange information through the OASIS3 coupler (Valcke, 2013).

The atmosphere model sends wind stresses on both water and ice, net precipitation less evaporation over water and ice, snowfall, evaporation over snow/ice, net shortwave flux, net non-solar heat flux, solar heat flux on ice, non-solar heat flux on ice, non-solar heat flux derivative.

The ocean model sends SST, sea ice, sea ice temperature, sea ice albedo.

To improve coupled model stability a correction can be applied to the heat flux from the ocean. The correction has been computed considering the difference between the ocean model output and the

required atmosphere model input to keep the simulation stable in reference conditions. More details about the flux correction can be found in (Kröger & Kucharski, 2011)

OASIS3 runs as a separate binary and performs synchronization and regridding. The coupling configuration is defined in a configuration file ("namcouple"). All processes are initially started and as a first step they setup the MPI (Forum, 1994) communication channels. Source and target grids are defined in auxiliary NetCDF files. For parallel models, such as NEMO, partitioning must be defined so that the coupler knows how to correctly position the data in the overall grid.

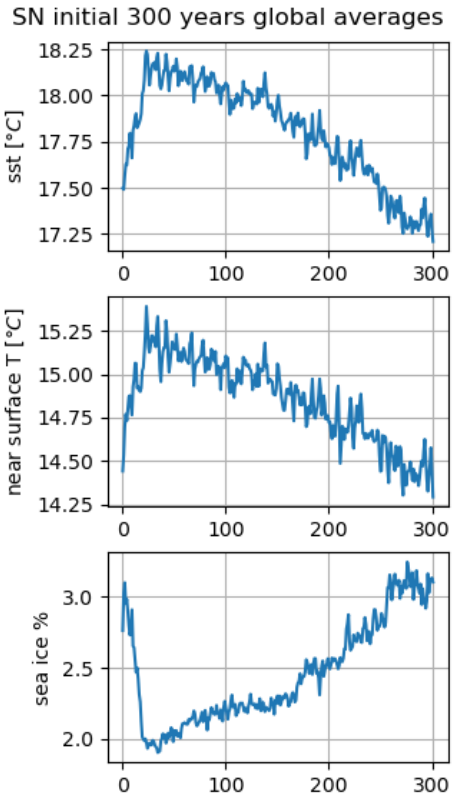

Figure 7 values from initial 300 years run. The values appear to stabilise after about 260 years.

Each process must declare which fields it sends or receives. The information in the namcouple file allows to complete communication and regridding setup. Communication is performed at model time steps. Each process only knows what information to send and what information it needs to receive, but not where the information is sent to and where it comes from.

Regridding is required to transfer the information from the source model grid to the target model grid. Many different options can be configured to handle scalar and vector 2D fields on a variety of grids (Valcke, 2013).

OASIS3 counts seconds to synchronize the models and schedule data exchange. Since a 32-bit signed integer is used for the counter the overall duration of a single simulation run is limited to slightly more than 68 years.

Figure 6 shows model scheduling and interaction through the OASIS3 coupler.

3. Methodology and Data

This section describes the methodology adopted to setup the model, to produce a long, coupled spin-up run to achieve a statistically steady state and to produce a simulation suitable for a validation of the model against observations of the recent past.

The correct execution of the code and the model restart methodology have initially been checked with short runs to exclude issues due to the porting of the software to the new environment.

A longer time span simulation has then been used to check that climatological stability had been reached. The simulation has been run applying a steady state forcing corresponding to conditions representative of the years 1980-2000.

The main variables from a long stretch of a climatologically stable simulation have finally been checked comparing them with ERA5 reanalysis and other data.

3.1. Test runs for the validation of the execution methodology

The first step has been to setup compile and link the model software on the University of Bologna High Performance Cluster (OPH Cluster). This entailed compiling and linking all the model components and some required libraries: NEMO, OASIS3, SPEEDY and the NetCDF library.

Initial checks simply concerned correct compilation and linking, execution without errors and no evident issues with the model output. The first complete model runs showed a very rapid freezing over of the planet that was later found to be linked with some changes in the Fortran language specification since the original code has been written. The issue was fixed with a compiler option.by adjusting accordingly the compiler options.

Checks for a consistent bit level reproduction of model simulations led to the discovery that the model produced different numerical results on different servers of the cluster, this is consistent with

the inhomogeneous architecture of the cluster. The execution of the model was therefore limited to a subset of the servers to have identical bit level results when starting from identical conditions.

With the current model configuration simulation duration is limited to slightly more than 68 years due to OASIS3 counting time in seconds in a 32bit signed integer. Longer simulation times can be obtained restarting the simulation from restart files written by the models.

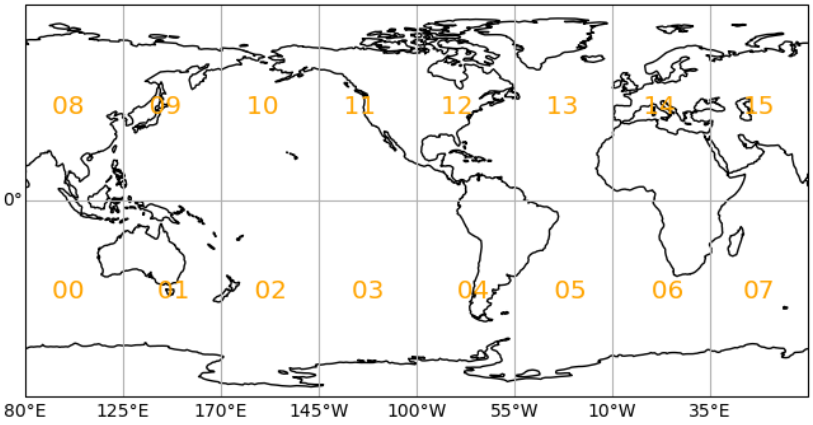

Figure 8 NEMO Ocean processor domains in a 8x2 configuration. Numbers identify output files (see Appendix). The map does not correctly represent partitioning where increased resolution is applied such as in the Mediterranean or Red seas.

The restart procedure was therefore checked in detail. This verification has led to a small modification of the previously implemented restart procedure to prevent an inconsistent initialisation of sea-ice cover at the restart (see paragraph 5.2 for a detailed description).

An analysis of the model performance and scalability has been performed, operating on the parallelisation of the ocean model. Both 8 and 16 processor ocean model configurations have been tested. The two configurations do not significantly differ in terms of computational speed, this can be explained by the fact that in principle more domains increase the communication computation requirements. However, the 16 processor NEMO configuration of the coupled model has proved more stable. In some 8 processors simulation runs the atmosphere component crashed. All simulations have therefore been run on a 16 processors configuration, with computational ocean domains defined as shown in Figure 8.

Specific tests on the restart procedure have confirmed that for this coupled model restarted simulations are not bit level compatible with continuous simulations, but statistical analyses on the model output led to the conclusions that this mismatch was not affecting the model climate. .

The std=legacy compiler option has become necessary after cluster GNU Fortran upgrade from version 8.3.0 to version 10.2.1 to bypass compilation errors.

3.2. Spin up Simulations, Stability Checks and Stationary Simulation for Model Validation

Once a stable configuration of the model and of the running environment was achieved, a long run with constant forcing was performed to evaluate and reach a statistically stable state. One of the tests runs described in the previous section was analysed for this purpose and indeed showed significant changes in key values characterising the model climate, such as sea surface temperature, near-surface air temperature and sea-ice cover, see Figure 7. A new run was therefore started from there and was progressively extended to 1020 until the key diagnostics, shown in Figure 9, showed a stable behaviour.

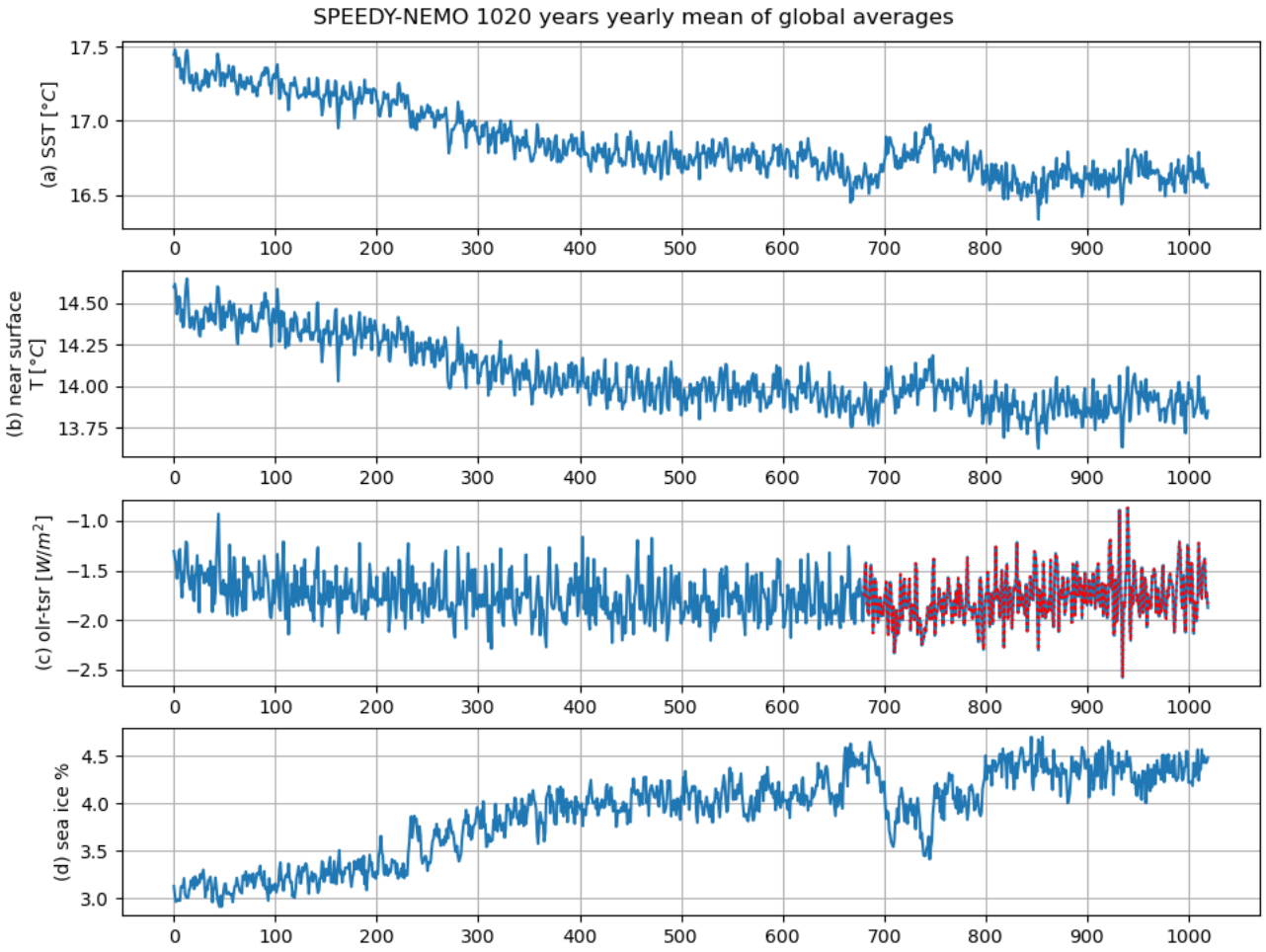

Figure 9 Yearly averages of global averages of some variables from the spin up run. The plot has been used to check whether the simulations had reached a steady state. The red dotted line in one of the plots shows the analysed period. olr-trs (outgoing long radiation -top of the atmosphere shortwave radiation) is a measure of the overall energy balance

The last 340 years which represents the stable state of the model have been retained for analysis and comparison with observations (see section highlighted in red in Figure 9 (c)). The overall spin up is therefore 940 simulation years long.

The plot marked "olr-trs" in Figure 9 (c) shows the overall energy balance (outgoing longwave radiation minus top of the atmosphere shortwave radiation). An energy imbalance of around 1.7 Wm^{-2} is evident. Possible reasons for this have been identified but not verified. Energy imbalances, however, are not uncommon and the value of 1.7 Wm^{-2} falls in the range exhibited by state-of- the-art-models (Wild, 2020)

SST data are stable over the 340 years of the run with good performance compared to other models like those studied in (Gupta, Jourdain, Brown, & Monselesan, 2013). Care must be taken, however, since the SPEEDY-NEMO run is shorter than most of the simulations analysed in the paper.

3.3. Data and Tools

ERA5 reanalysis data have been used as a reference for atmospheric variables. The data has been generated using Copernicus Climate Change Service information 2021

For surface variables: SST, 2m temperature, mean sea level pressure and total precipitation see: (Hersbach, et al., 2019)

For upper air variables: meridional velocity, zonal velocity, geopotential height and temperature, see: (Hersbach, et al., 2019)

NOAA_ERSST_V5 data provided by the NOAA/OAR/ESRL PSL, Boulder, Colorado, USA, from their Web site at: https://psl.noaa.gov/data/gridded/data.noaa.ersst.v5.html#detail

NSIDC sea ice extent data have been extracted from: Gridded Monthly Sea Ice Extent and Concentration, 1850 Onward, Version 2 - https://nsidc.org/data/G10010/versions/2 (Walsh, Chapman, & Fetterer, 2019)

SPPEDY-NEMO and other data sources NetCDF files have been processed with Climate Data Operators - CDO (Schulzweida, 2020)

Plots have been made using Python3 (Van Rossum & Drake, 2009), matplotlib (Caswell, et al., 2021) and Cartopy (Met Office, 2010 - 2015)

4. Results

In this section, the model has been validated comparing results to observed and reanalysis datasets on annual and seasonal timescales for surface as well as for upper atmosphere variables. It is important to mention, that the 340 years validation run, used in all comparisons, was carried out with steady state forcings tuned to the years 1980-2000

4.1. Validation of Surface Variables

In this section, the validation of the surface features of the models has been shown. Mainly the Sea Surface Temperature (SSTs), Near-surface Air Temperature (also known as 2m-air temperature), Precipitation and Mean Sea Level Pressure have been evaluated.

SST has been compared to ERA5 reanalysis data (Hersbach, et al., 2019) and NOAA Extended Reconstructed Sea Surface Temperature (SST) V5 (Huang, et al., 2017), see Figure 10
SPEEDY-NEMO SST data are stable and match reasonably well with measurements from the target simulation dates (1980-2000). Data above 60° N and below 60° S have been excluded from the averages since ERA5 data provide the temperature at the water-ice interface where sea ice is present, while SPEEDY-NEMO reports the temperature at the ice-atmosphere interface. The model

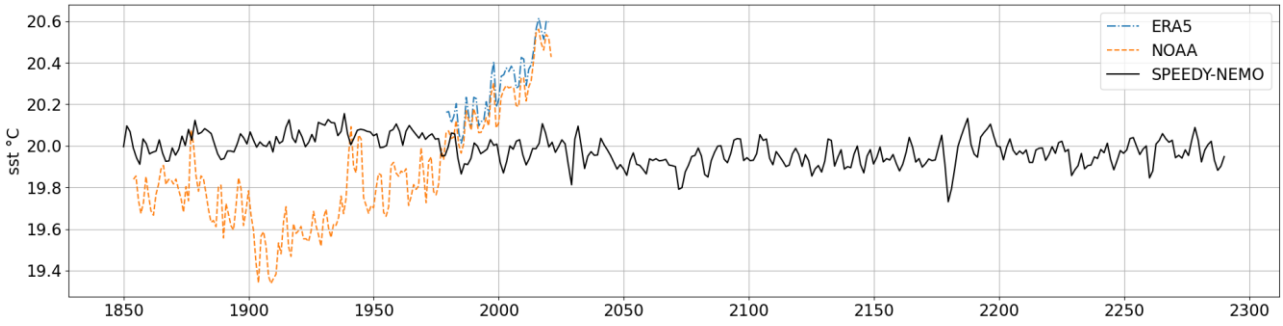

Figure 10 SPEEDY-NEMO global yearly average SST compared with NOAA and ERA5 SST. Data between ± 60° N only

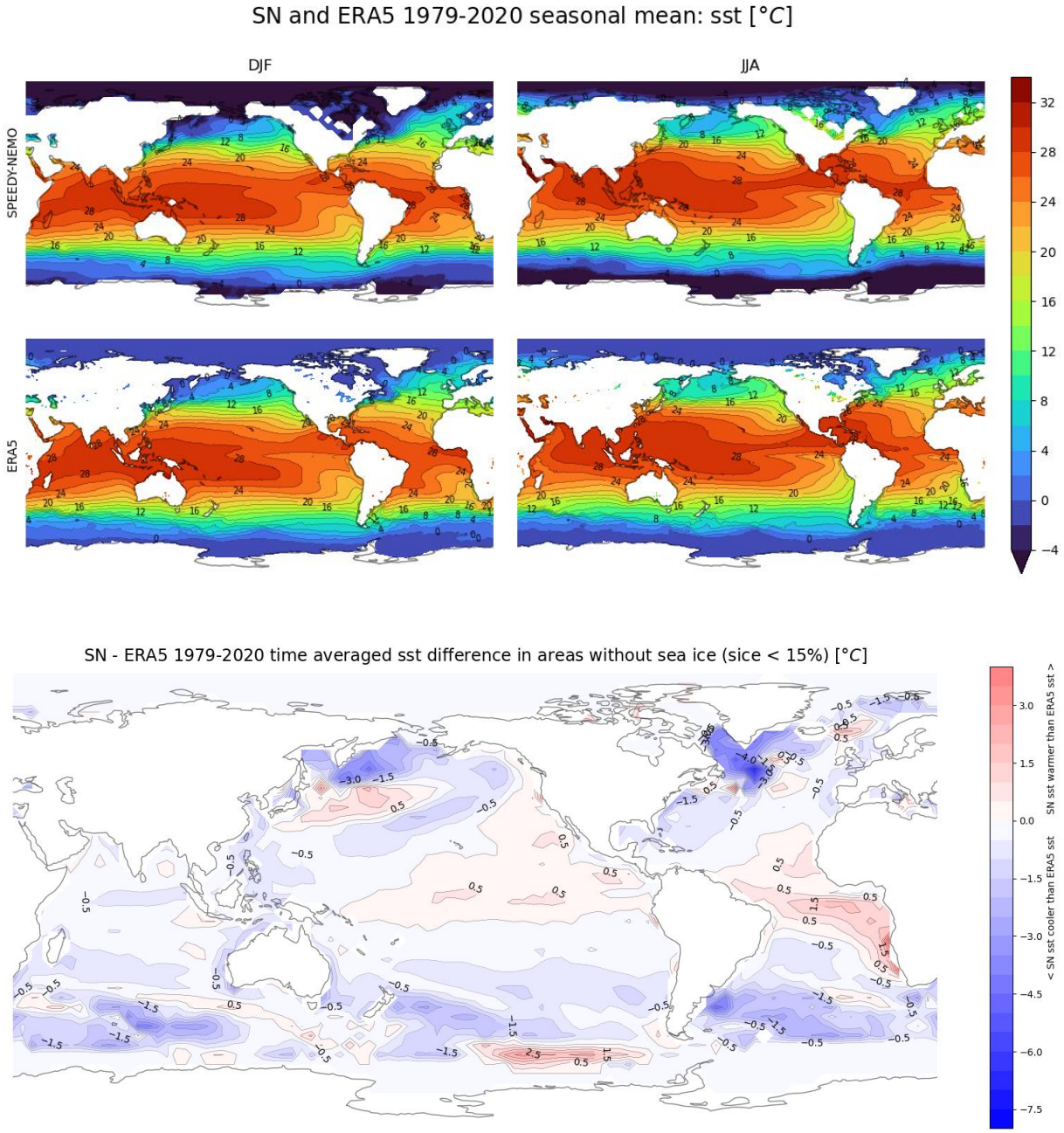

Figure 11
Top: SPEEDY-NEMO and ERA5 seasonal mean SST. The two data sets provide different values where sea ice is present. ERA5 SST is the water temperature at the water-ice interface, SPEEDY-NEMO SST is the temperature at the ice atmosphere interface. Due to this the temperature difference in the polar regions is out of the displayed range.
Bottom: difference between average SPEEDY-NEMO SST and ERA5 (1979-2020) SST. Areas with more than 15% sea ice have been masked out

has a lower variability than real world data. This is probably due to the model not including processes that impact climate variability like stratospheric aerosols and volcanic eruptions.

Figure 11 shows the seasonal average of the Sea Surface temperatures (SSTs) from SPEEDY-NEMO and reanalysis/observations dataset (ERA5) 1979-2020 data, for the boreal winter (DJF) and the

boreal summer (JJA) season. SPEEDY-NEMO reproduces reasonably well the spatial seasonal mean SSTs across the globe compared to the observations, but with some biases. Figure 11 bottom shows the mean SST biases between the SPEEDY-NEMO and ERA5 averaged over the whole period. Areas where sea ice covers more than 15% of the surface have been masked out due to the different temperatures provided by the two data sets. The main differences are close to the southwestern Africa coast where SPEEDY-NEMO SST show warm biases compared to the ERA5 temperatures and in the Labrador region where the opposite is true (I.e., the cold biases).

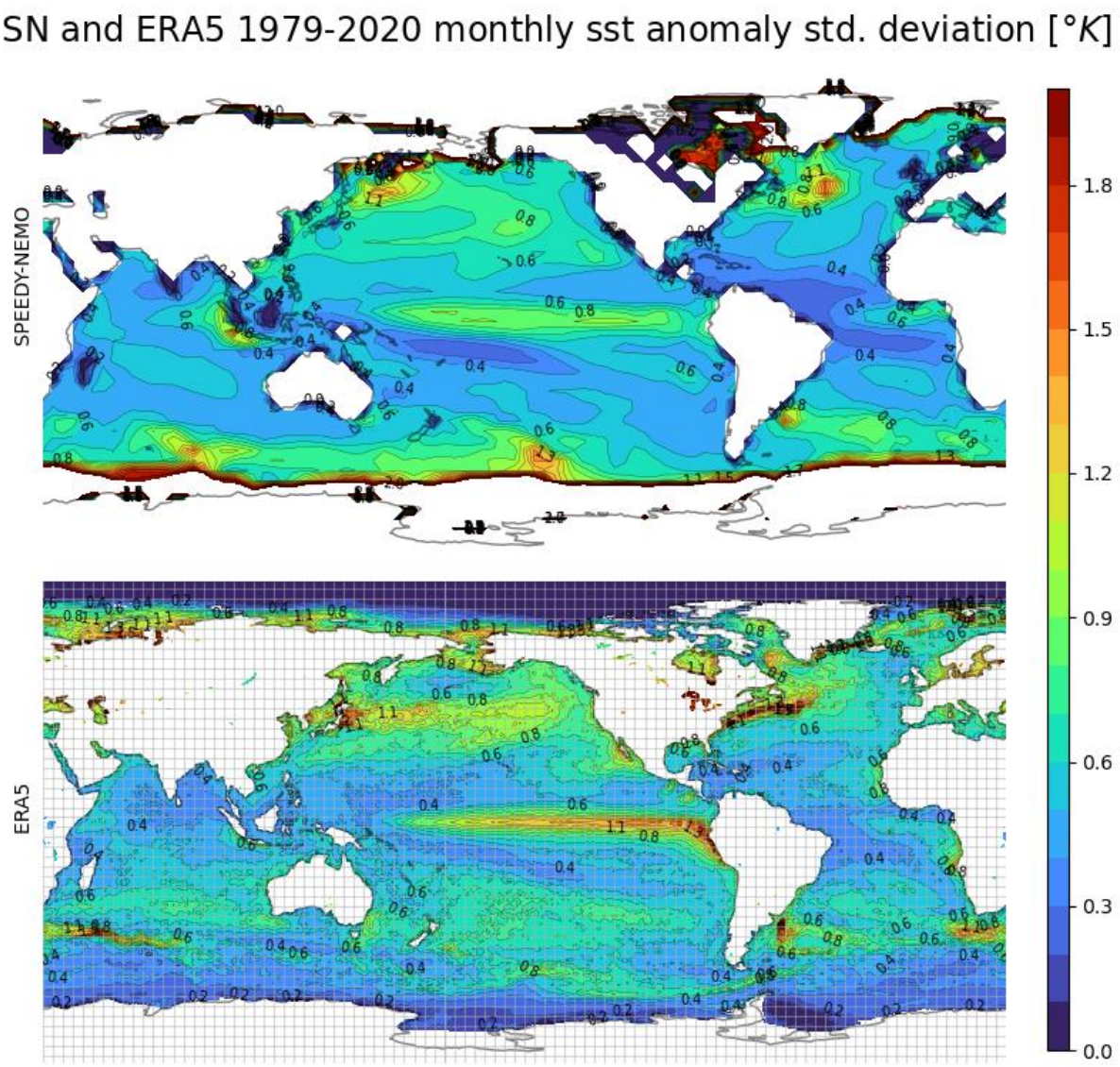

Figure 12 SPEEDY-NEMO and ERA5 standard deviation [°K] of the difference between monthly average SST and average monthly climatology. The El Niño signal is clearly visible in the SPEEDY-NEMO data even though less sharply than in the ERA5 data. SPEEDY-NEMO

The SST variability is defined as the square root of the mean square anomaly. The annual cycle of the SST variability has been analysed after removing the seasonal cycle from the SPEEDY-NEMO and ERA5 data. Figure 12 shows the SST variability for both SPEEDY-NEMO and ERA5 reanalysis data.

The SPEEDY-NEMO atmospheric model grid has been added to the ERA5 plot to show the proportion between the grid and the phenomenon to be simulated. It must be noted that the SPEEDY-NEMO atmosphere grid has a 96x48 resolution, while ERA5 data have a 1440x720 resolution. Model tends to simulate the spatial SST variability quite well compared to the observations, where the highest signal is in the tropical region with a maxima in the equatorial pacific region, which is the El Niño-Southern Oscillation (ENSO) region. Model can capture the tropical Indian Ocan as well as the tropical Atlantic mode quite well but with weaker magnitude compared to the observations. The SPEEDY-NEMO signal is less sharp and weaker close to the South America coast compared to the observations. It shows that model has an ability to be used to understand the climate mode and its interaction with atmosphere, which will be carried out in detail in the future studies. The polar areas where sea ice is present have been excluded from the SPEEDY-NEMO plot since SPEEDY-NEMO reports SST at the air ice interface when sea ice is present and this has a very large variability compared to other areas. Overall, the model has a comparative and weaker variability than the observations/reanalysis. This is likely due to the model not including processes that impact climate variability such as stratospheric aerosols due to volcanic eruptions.

Figure 13 Shows the comparison of SPEEDY-NEMO simulated near Surface Air Temperature (SAT) also known as the 2m-air temperature (temp0) with ERA5 SAT for the boreal winter (DJF) and boreal summer (JJA) seasons. Overall, SPEEDY-NEMO SAT spatial seasonal mean distribution is in good agreement with observations with some notable biases over the land regions. Arid areas winter temperatures are lower than in the surrounding areas..

The SPEEDY-NEMO temperature distribution matches reasonably well averaged ERA5 data in both distribution and values. The only notable exceptions are over the North America during winter where SPEEDY-NEMO shows a warm temperature bias compared to the ERA5, which requires further investigation as of future work. Furthermore, the annual mean temperatures biases show a similar spatial distribution (Figure 14) compared to that of the seasonal mean biases (Figure 13). Overall, the biases are comparable to any state-of-the-art model (Stouffer, Hegerl, & Tett, 2000), which shows that model reasonably performs well in simulating the global surface air temperature.

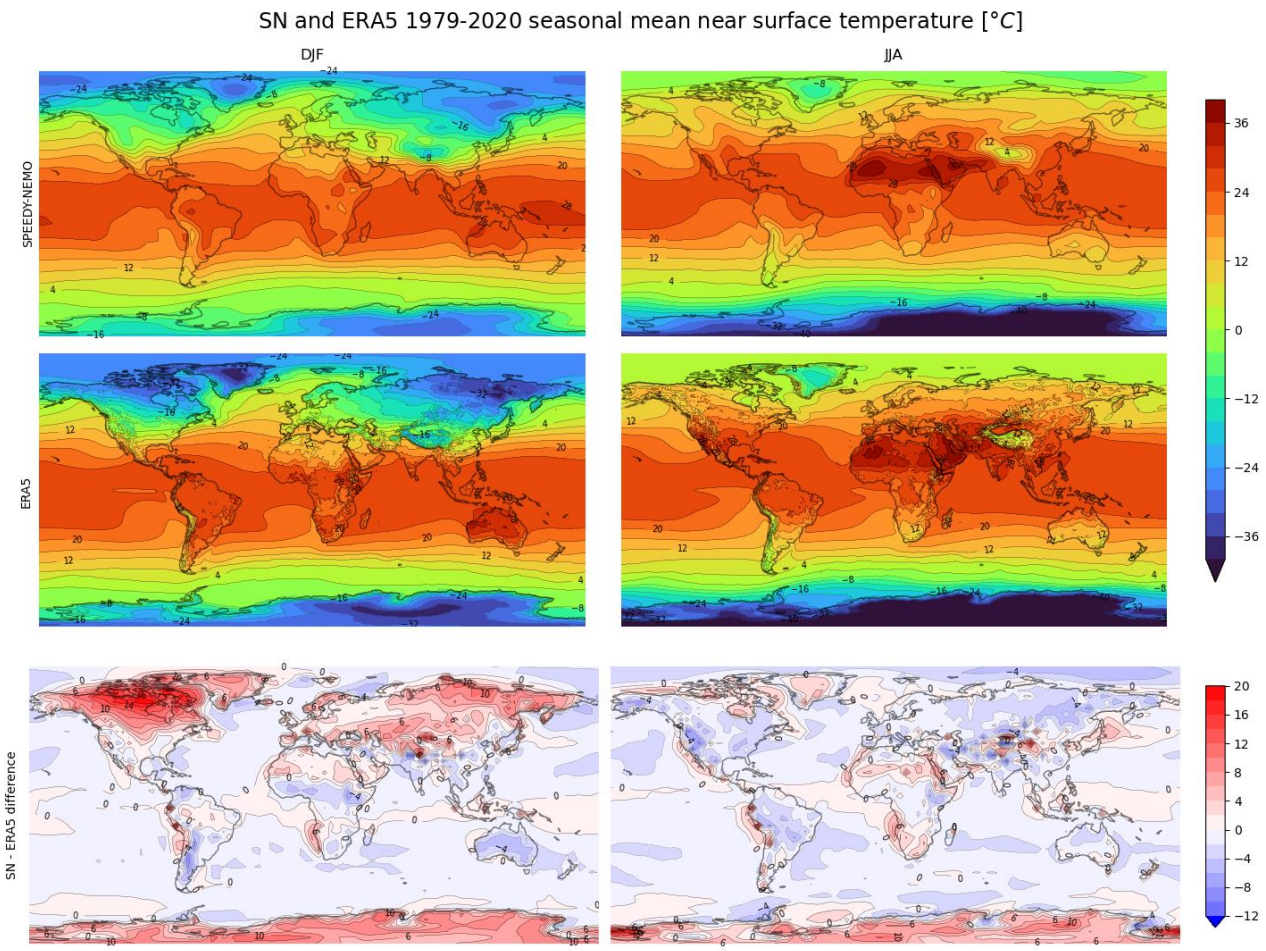

Figure 13 seasonal average comparison between SPEEDY-NEMO near surface temperature and ERA5 t2m temperature. Units are (°C)

Seasonal global precipitation patterns for the boreal winter (DJF) and boreal summer (JJA) from SPEEDY-NEMO and ERA5 are shown in Figure 15 and Figure 16. SPEEDY-NEMO and ERA5 maps have very different spatial horizontal resolution, where SPEEDY is on 96x48 against the ERA5 1440x720, which means each SPEEDY-NEMO grid element corresponds to 15x15 ERA5 grid elements. Therefore, ERA5 higher precipitation amount is due to its higher resolution which may favour the localized high rainfall

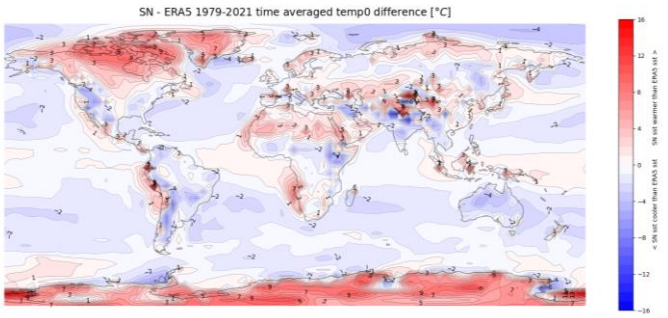

Figure 14 Annual mean biases (°C) of the SPEEDY-NEMO near Surface Air Temperature (SAT) compared to the ERA5 for the period 1979-2021.

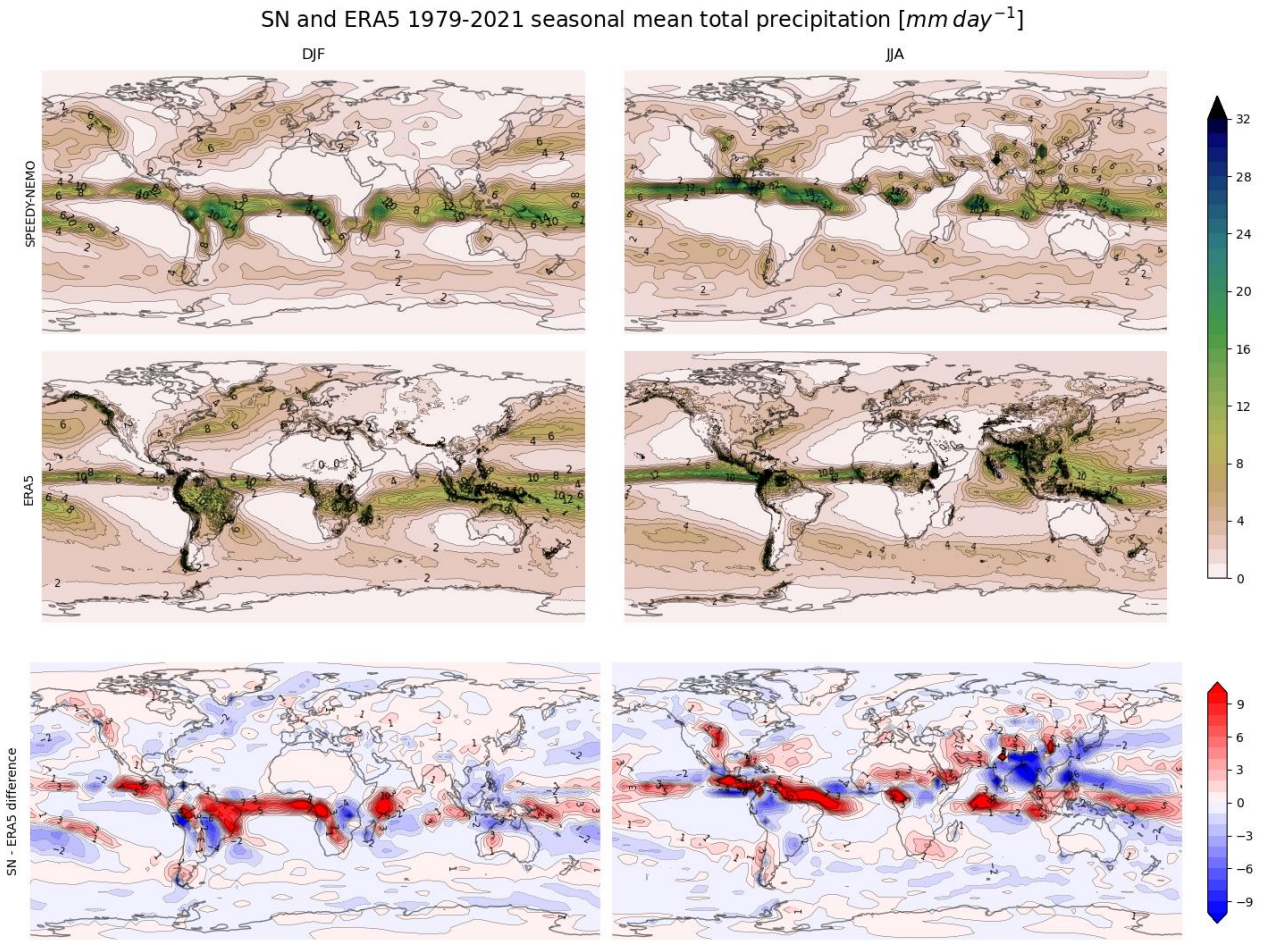

Figure 15 Seasonal mean precipitation for the boreal winter (DJF) and boreal summer (JJA) for the SPEEDY-NEMO coupled simulation compared with the Observed (ERA5).

compared to the coarser resolution of SPEEDY.

ERA5 data has been remapped to the lower SPEEDY-NEMO resolution to produce the comparison in Figure 15

Overall SPEEDY-NEMO seasonal rainfall spatial pattern corresponds well with the ERA5 data with maximum rainfall in the tropical regions. The tropical rain band moves north in summer and south in winter, which matches reasonably well with ERA5 data. During boreal summer (JJA) season, one of the main rainfall features in the northern hemisphere is the South Asian monsoon, which is simulated quite well in term of its spatial distribution although the magnitude is weaker. This weaker magnitude is mainly due to the model coarser resolution.

The global seasonal rainfall biases for the model with respect to the ERA5 is shown in Figure 15 bottom. Regional rainfall patterns correspond to ERA5 reanalysis in some areas and show some differences in other areas (see bottom plots in Figure 15). It matches reasonably well over the

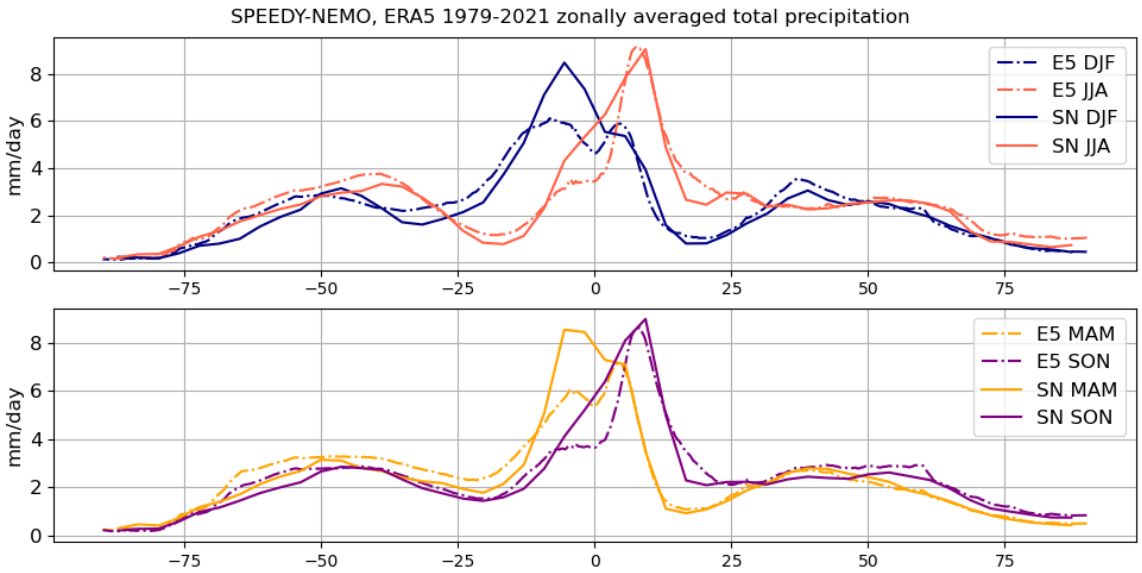

Figure 16 SPEEDY-NEMO and ERA5 1979-2020 zonally averaged total precipitation comparison. The match between simulation and reanalysis data is reasonably good in both distribution and amount. X-axis corresponds to the Latitudes.

Australian continent. SPEEDY-NEMO underestimates summer rainfall on India, Southeast Asia and Pacific equatorial south America, which represent the dry biases in these regions, while overestimation of the rainfall is noted in the equatorial Atlantic south America. SPEEDY-NEMO also overestimates rainfall on some arid areas, such as southern Sahara and Arabian Peninsula.

To analyse the seasonal migration and the latitudinal variation, the rainfall zonal mean across the globe is shown in Figure 16 The match between simulation and reanalysis data is reasonably good in both distribution and amount. Tropical summer distribution average is slightly shifted to the south as can also be seen in the SPEEDY-NEMO – ERA5 comparison map.

Mean sea level pressure results are compared to ERA5 data in Figure 17

SPEEDY-NEMO data show pressure field features like the summer high pressure fields over the oceans close to the eastern boundary of the basins and the winter Aleutian and Icelandic lows.

The overall pressure distribution for both summer and winter corresponds reasonably well to ERA5 data as can be seen in the bottom plots. The lower SPEEDY-NEMO winter pressure over north America is consistent with the higher temperature that can be seen in Figure 13

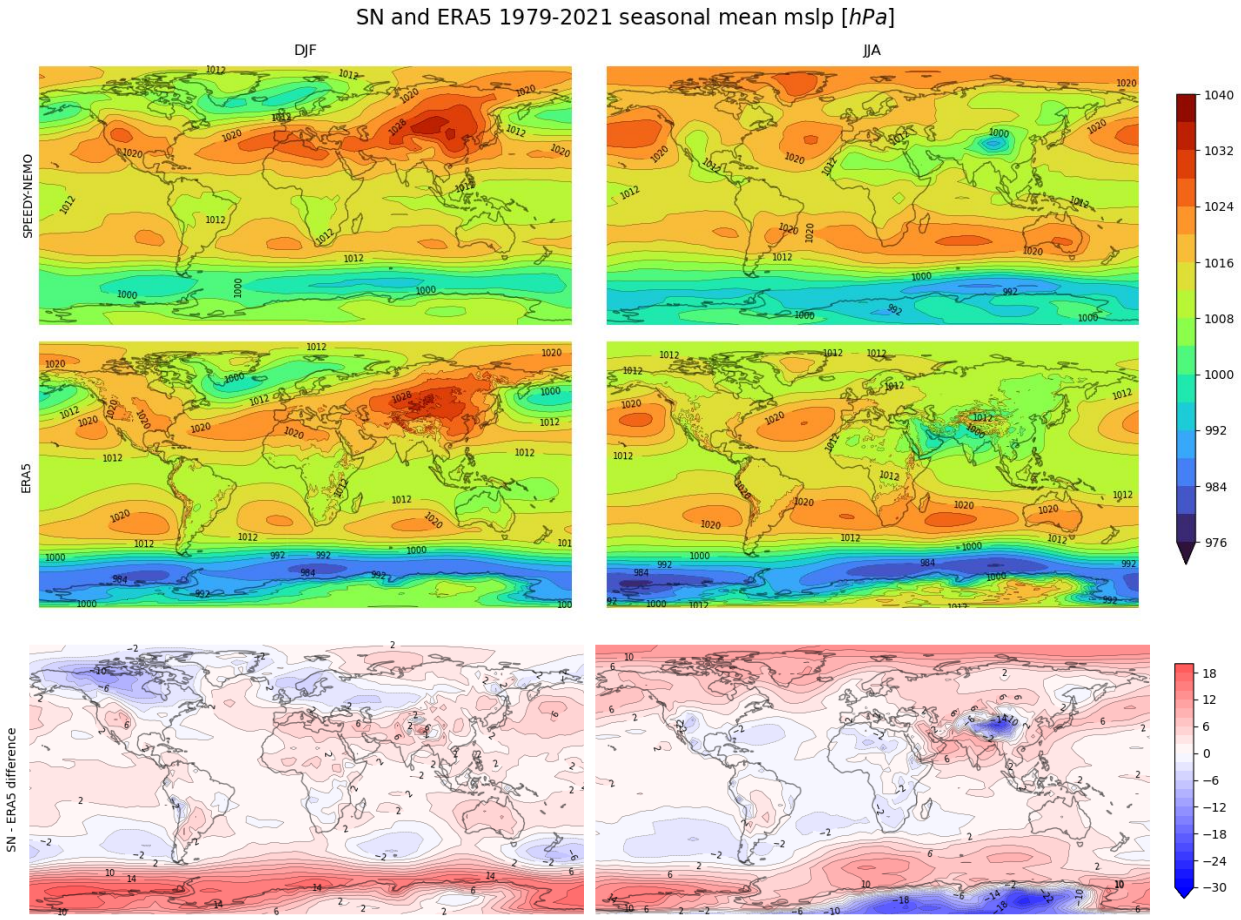

Figure 17 SPEEDY-NEMO and ERA5 seasonal average mslp. SPEEDY-NEMO high and low mslp distribution matches reasonably well with reanalysis data with somewhat larger differences in the polar regions

4.2. Validation of the Mean Atmospheric Circulation

In this section, the atmospheric circulation response of the SPEEDY-NEMO coupled model is analysed in comparison to the fifth-generation European reanalysis dataset (ERA5). Figure 18 shows the mass streamfunction, computed from the zonal mean of the meridional component of the wind for the boreal winter (DJF) and the boreal summer (JJA) seasons. The meridional structure is quite well simulated by the SPEEDY-NEMO compared to the observations but with weaker magnitude. The Hadley and Ferrel cells are reasonably like ERA5 results in both position and transport magnitude. It shows that the model captures the main dynamical features quite well even with the

coarser resolution. The coarser resolution mainly affects the model simulated magnitude, but the main features are still comparable with the observations as shown in Figure 18

Another important feature for the model to be well simulated is the location of the jet stream, which is one of the main features which modulate the extratropical weather and the climate system, particularly during the winter season. Therefore, the zonal mean of the zonal winds was analysed for the winter and summer season as shown in Figure 19. The hemispheric seasonality of the jet stream is quite well reproduced, where the maximum is appeared in the boreal winter (DJF) season in the northern hemisphere, while the southern hemisphere shows the maximum mean response in boreal summer (JJA), which is the winter for the southern hemisphere. The jet stream positions in Figure 19 correspond, as expected, to the boundary between the Hadley and Ferrel cells. Jet streams get stronger in winter due to the larger temperature gradient.

Figure 20 shows 200 hPa zonal winds for both ERA5 and SPEEDY-NEMO for the boreal winter and summer seasons. During the winter season, the stronger jet currents are noted in the northern hemisphere in the extratropical regions in the model, the spatial distribution is comparable to the observations but with weaker magnitude. Figure 20 is consistent with the position of the jet stream maximum in the high latitudes. The weaker magnitudes are due to the model coarser resolutions compared to the observations.

Figure 21 shows the seasonal average geopotential height variance, which represents the storms. Monthly values are computed considering all timesteps. The storm tracks, where midlatitude cyclones are more frequent, can be clearly seen over the oceans in the north hemisphere. Around the South pole they are almost continuous since there is very little land at their latitude.

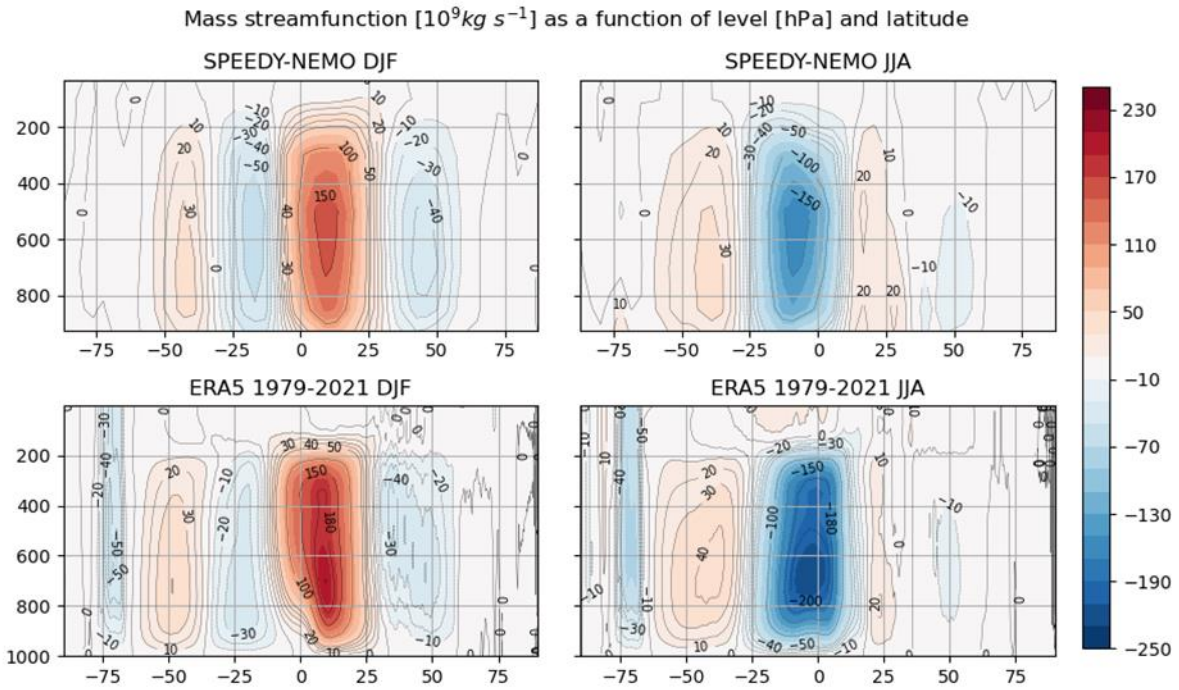

Figure 18 SPEEDY-NEMO and ERA5 1979-2021 seasonal mass streamfunction

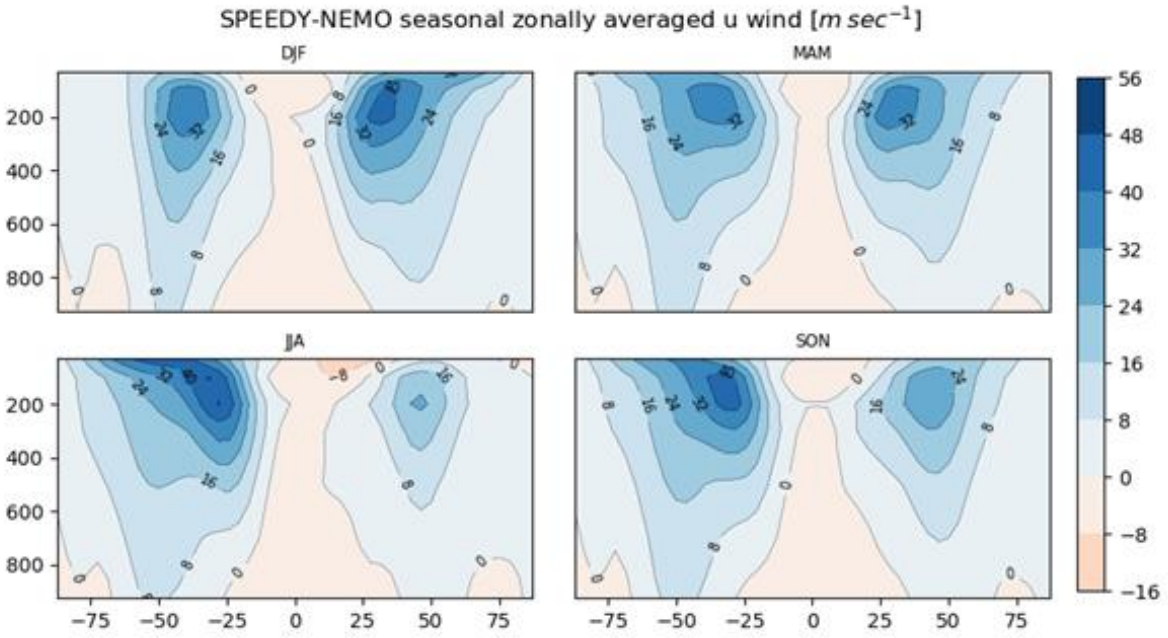

Figure 19 SPEEDY-NEMO zonal average of the seasonally averaged u wind. The jet streams and their seasonal changes are clearly visible

4.3. Sea Ice Validation

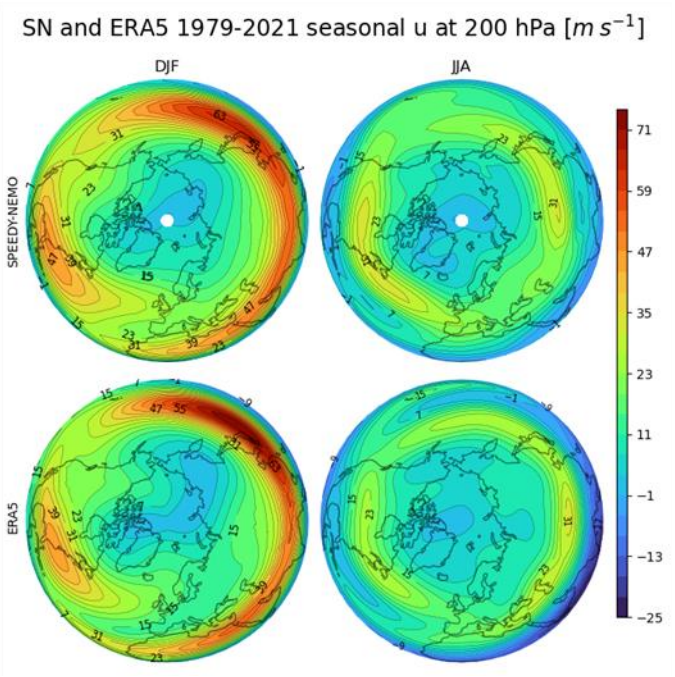

Figure 20 Polar stereographic Projections for the SPEEDY-NEMO zonal wind with the ERA5 at 200-hPa level. Unit s are (m/sec)

Sea ice melts and forms with the changing of the seasons. Arctic sea ice only partially melts each summer while most of the Antarctic Sea ice melts and reforms each year. Sea ice affects heat and moisture exchange between sea and atmosphere and ocean salinity in the polar regions. Sea ice is not unbroken. Cracks, called leads, open due to mechanical stress and differences in velocity between different sea ice areas. Two measures are usually given of the area covered by sea ice: ice area, which is the ocean surface effectively covered by ice where at least 15% of the ocean surface is occupied by ice and ice extent which is the area of all the grid cells where the cover is at least 15%

SPEEDY-NEMO sea ice modelling has been checked comparing the average monthly arctic sea ice extent with historical data from the National Snow and Ice Data Center (NSDIC), see (Walsh, Chapman, & Fetterer, 2019).

As shown in Figure 22 the model reproduces maximum and minimum total northern hemispheric sea ice extent well. Also the spatial distribution of average maximum and minimum sea ice extent is well reproduced when compared with the observed

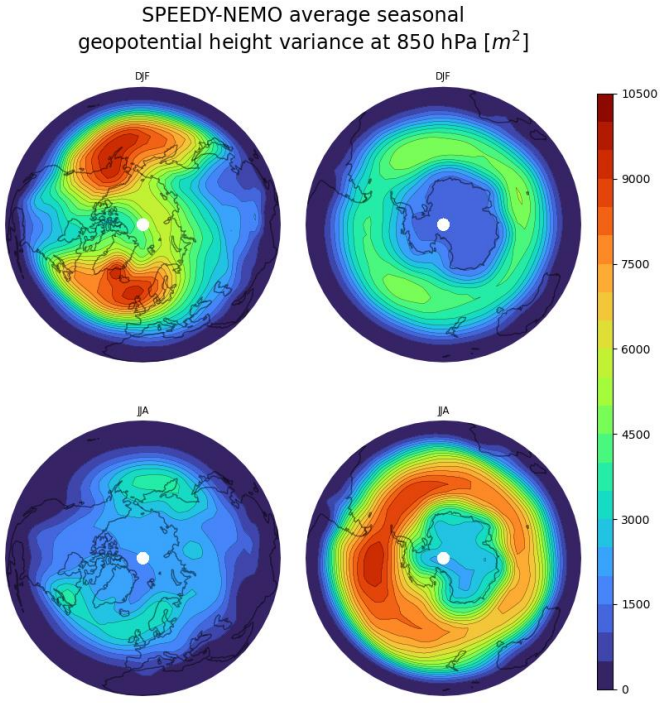

Figure 21 SPEEDY-NEMO Lower-level geopotential height variance at 850 hPa level with the polar stereographic projections for the North and South poles plotted

distributions in 1980 with some local details missing in the SPEEDY-NEMO simulation due to the relatively coarse model resolution.

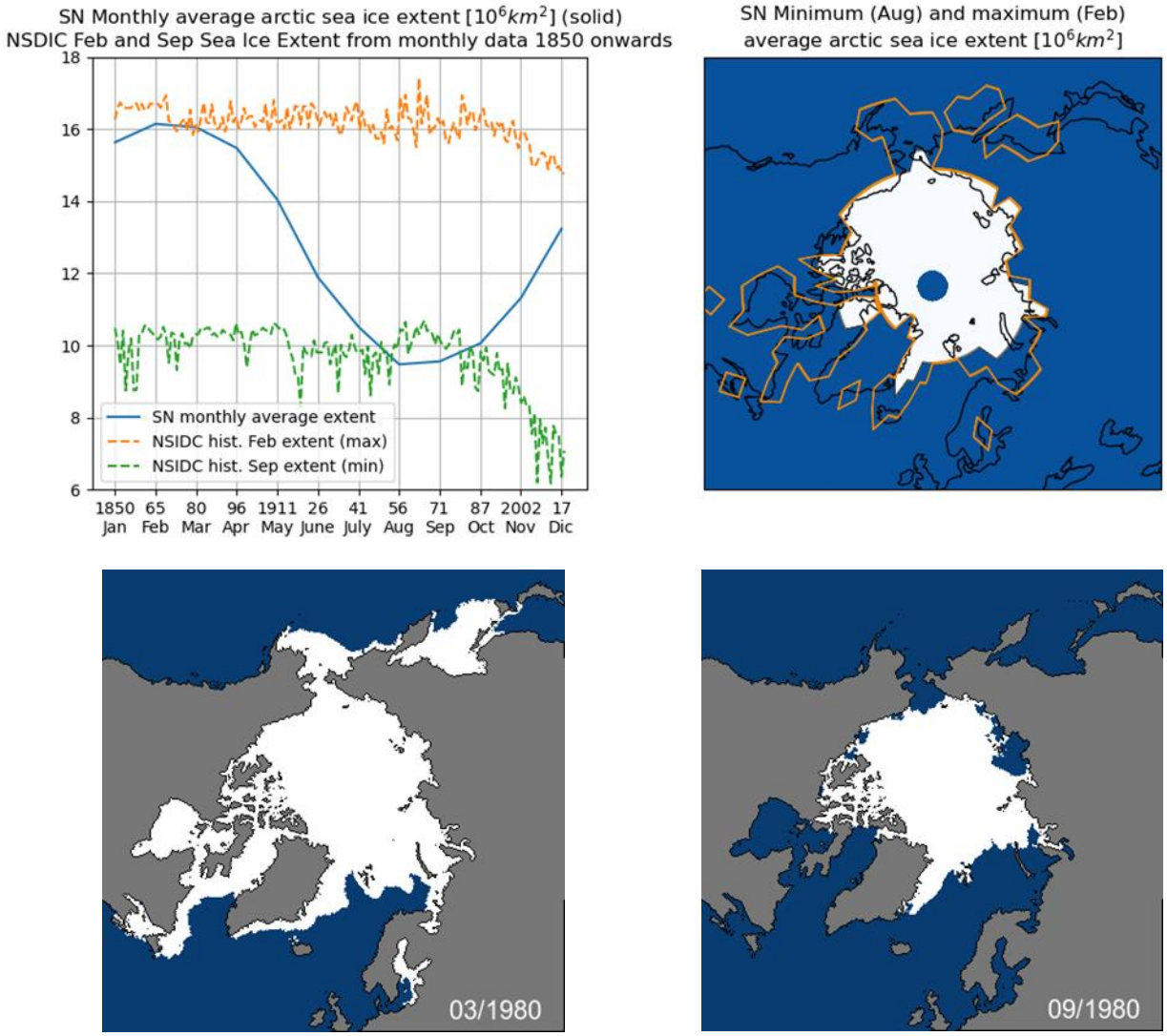

Figure 22 Top: sea ice extent. Average model results on the whole 340 years run compared with NSIDC historical data. The data fits the minimum and maximum extents for the given forcings. The NSIDC historical data for mid February and mid September are plotted. These two months are close to the maximum and minimum extents. The plot on the map shows the model sea ice distribution corresponding to February and August of the plot on the left.
Bottom: sea ice extent NSIDC images from satellite data.

5. Technical Details

The software has been setup starting from a kit received from ICTP. The kit included all the sources for the models, the coupler and the postprocessing tools, a set of restart files tuned to conditions prevailing around 1980 and the scripts required to build and run the software modules and to postprocess outputs.
The kit also included instructions on how to port the software to a new environment and examples of scripts tuned to different build and execution environment.

The model has been run on the University of Bologna DIFA (DIpartimento di Fisica e Astronomia) cluster in the following environment:
Kernel: Linux
kernel-release: 5.10.0-10-amd64
kernel-version: #1 SMP Debian 5.10.84-1 (2021-12-08)
machine: x86_64
operating-system: GNU/Linux
MPI version is Open MPI: 4.1.0
NetCDF version: netCDF 4.7.4
C compiler: gcc version 10.2.1 20210110 (Debian 10.2.1-6)
Fortran compiler: GNU Fortran (Debian 10.2.1-6) 10.2.1 20210110

The main modules of the model are the AGCM SPEEDY, the ocean model NEMO and the coupler OASIS3. The software requires the NetCDF (Network Common Data Form) library for file I/O and the MPI library for interprocess communication.
Compilation of the modules and model running are driven by script files available in the received kit. The scripts and options, originally written to use Intel compilers and linkers, have been modified to run on the OPH cluster (Debian) environment adapting the directory structure and changing compilers, linkers and build options to fit the new environment.

All components should be compiled with the same compiler and linked to the same library versions to prevent problems. OASIS3 need only be recompiled if the environment changes, NEMO must be recompiled to change the domain parallelization setup and SPEEDY is recompiled and linked at each run.

5.1. Running the Simulations

Simulations with Speedy-Nemo require an initial state of the ocean and of the atmosphere to be set. The initial state is retrieved from a set of restart files generated by a previous run.

Each run produces a set of output files for the atmosphere and multiple sets of output files for the ocean, one for each domain in which the oceans have been subdivided. SPEEDY outputs GRIB files while the ocean model generates NetCDF files.

Restart files are in a program specific format for SPEEDY and in NetCDF format for NEMO. The NEMO restart files and output files are partitioned into domains. NEMO restart files must be reassembled into a single restart file to be used. The s/w kit includes a tool (rebuild) to reassemble the domain output files into global files.

The file time.step in the output folder shows the current time step and can be used to monitor progress. One year of simulation has 5475 steps with the setup we used. An 8x2 68 years simulation takes approximately 20 hours on a server equipped with an Intel(R) Xeon(R) Gold 5120 CPU @ 2.20GHz and generates about 53Gb of output data. It requires 18 processors: 1 for SPEEDY, 1 for OASIS3 and 16 (8x2) for NEMO and runs on 5 Gb of RAM.

The logic of the scripts available in the ICTP kit to compile the programs and run the simulation have been slightly modified and new scripts have been prepared to automate compilation execution and restart of SPEEDY-NEMO.

As mentioned in 0, only slightly more than 68 years can be simulated in a single run. If longer times are required, the simulation must be restarted from the final state saved by a pervious run. The ocean model generates the restart files before the end of the year while the ice model produces its restart files at the beginning of the new simulation year even though all the restart files refer to the same end of year time step. The simulation must, therefore, continue after the required duration to generate all the restart files.

In addition to the final restart files the models generate intermediate restart files that can be used if the run does not complete for any reason.

The simulation can be restarted at any time step for which a full set of restart files is available. We have been running 68 years plus one month simulations so as to be able to restart after 68 years (372300 steps).

Consecutive run output files can be spliced together to produce output files that span more than 68 years.

Restarting the simulation to produce long runs requires

- Rebuilding NEMO restart files from the domain files
- Copying SPEEDY restart file in the SPEEDY setup directory
- Copying the sstocean file from the previous run to the restart directory

To reassemble outputs in NetCDF format

- SPEEDY output must be converted to NetCDF for example with cdo import_binary
- NEMO output files must be rebuilt from domain files
- any duplicate records that have been generated to get the ice model output must be removed
- the simulation segments must be assembled into single files with tools like cdo -mergetime

5.2. Solved Problems

The first simulations showed a very rapid ocean ice over This issue has been traced to a change in floating point zero representation since the original code has been written. Following IEEE 754 standard zero has become a signed quantity.

The code in lim_thd(kt) subroutine computes a mask to check for sea ice with the following statement:

```
zindb = tms(ji,jj) * ( 1.0 - MAX( zzero , SIGN( zone , - zthsnice ) ) )
```

which does not produce the correct result if zero is negative. The issue has been solved with the "-fno-sign-zero" compiler option.

During restart testing we noticed a big (4 °K) near surface temperature step at 80 N between the ending and restarting simulations. This was due to a reset of the sea ice in the first (00) ocean

domain at restart. The issue was very visible during the initial test runs that covered the whole earth with a single domain. With more domains the first domain (see Figure 8) is usually in the southern hemisphere and the January restart is in the austral summer. The effect on sea ice is therefore absent or very limited.

The issue is due to a reinitialization of a variable which has already been loaded with the restart information. The code in subroutine cpl_prism_define () performs the initialization only if the file sstocean from a previous run is not available. To solve this issue the restart procedure has been modified to retrieve the sstocean file from the previous run.

6. Conclusion

Intermediate complexity atmosphere and ocean general circulation models offer significant opportunities to explore a wide range of climate related phenomena and interactions: they allow to examine low- and ultra-low- frequency variability in long simulations; they can provide robust statistical samples by enabling massively large ensemble simulations; they offer a flexible framework to test hypotheses under a range of assumptions on model parameters and complexity. This work has addressed the validation of a new intermediate complexity, fully-coupled climate model based on a set of existing atmosphere, ocean and sea-ice models. A first part of the study, that leveraged on an existing modelling suite, focused on the preparation of the environment and the debugging of the coupling and restarting procedure. A second part of the work has been devoted to the execution of a spin-up run to achieve stability, a present-climate run with prescribed constant forcing and a comparison of the latter with observations and reanalyses of the recent past.

The initial validation of SPEEDY-NEMO has shown that the model can be ported to a new server with limited effort and that long simulations spanning a thousand years can be easily run. The model runs on limited h/w resources and therefore significant size samples can be generated if needed

Our results prove that long timescale, stable simulations are feasible.

SPEEDY-NEMO reproduces important features of Earth mean climate and variability, despite the use of a fairly limited resolution grid, simple parameterizations and a limited range of physical processes is accounted for. SST distribution is quite similar to ERA5 reanalysis SST, in tropical and mid latitude areas the difference is within ± 0.5 °K. El Niño like SST variability, displayed by the model after almost 1000 years of free running, shows the reasonably good performance of the atmosphere and the ocean models and of their coupling. Precipitation distribution is also similar to reanalysis data even though condensation and precipitation processes are parametrized in the model. Total precipitation is within ± 50% of reanalysis data except on equatorial Atlantic Ocean and in other very localized aeras.

Wind and pressure distributions show the main features of Earth climate such as jet streams and winter storm tracks over the oceans and stationary high and low pressures. Hadley and Ferrel cells are clearly displayed by the mass streamfunction and the transport has reasonable values.

Sea ice modelling generates minimum and maximum arctic sea ice extents and ice distributions similar to the measured values.

Ocean model outputs have not been assessed even though SST data, El Niño signal and arctic sea ice show that ocean model behaviour is close to what we expect.

The results show that SPEEDY.NEMO is a promising tool for climate studies, but to understand SPEEDY-NEMO full potential the validation should be improved and extended with an analysis of ocean variables and targeted simulations with modified conditions to check model behaviour under different conditions.

Changes in the parameters and the flexibility in parametrization have not been explored and more knowledge about these aspects would complete the picture.

From the model execution point of view overcoming the 68 years limitation would make SPEEDY-NEMO much more practical for runs longer than 68 years.

7. Acknowledgements

I would like to thank my dissertation supervisor Dr. Paolo Ruggieri for ins insightful supervision and continuous support. I also wish to thank all co-supervisors: Dr. Salvatore Pascale for his many useful suggestions and for pushing me forward with renewed challenges. A Great thanks to Dr. Fred Kucharski who made the model available and unfailingly supported me on making it work explaining its operation and analysing the results and to Dr. M. Adnan Abid who prepared the sw kit and the setup instructions and provided a lot of advice particularly in the final phases of the work.

8. References

Abid, M., Kang, I.-S., Almazroui, M., & Kucharski, F. (2015, November). Contribution of Synoptic Transients to the Potential Predictability of PNA Circulation Anomalies: El Niño versus La Niña. *Journal of Climate, 28*, 8347-8362. doi:10.1175/jcli-d-14-00497.1

Barimalala, R., Bracco, A., & Kucharski, F. (2011). The representation of the South Tropical Atlantic teleconnection to the Indian Ocean in the AR4 coupled models. *Climate Dynamics*.

Bourke, W. (1974). A multi-level spectral model. I. Formulation and hemispheric integrations. *Monthly Weather Review, 102*, 687–701.

Caswell, T. A., Droettboom, M., Lee, A., De Andrade, E. S., Hoffmann, T., Hunter, J., . . . Ivanov, P. (2021). matplotlib/matplotlib: REL: v3.5.1. *matplotlib/matplotlib: REL: v3.5.1*. Zenodo. doi:10.5281/ZENODO.5773480

Cavalieri, D. J., & Parkinson, C. L. (2012, August). Arctic sea ice variability and trends, 1979–2010. *The Cryosphere, 6*, 881–889. doi:10.5194/tc-6-881-2012

Claussen, M., Mysak, L., Weaver, A., Crucifix, M., Fichefet, T., Loutre, M.-F., . . . Wang, Z. (2002, March). Earth system models of intermediate complexity: closing the gap in the spectrum of climate system models. *Climate Dynamics, 18*, 579–586. doi:10.1007/s00382-001-0200-1

Ehsan, M., Kang, I.-S., Almazroui, M., Abid, M., & Kucharski, F. (2013, August 4). A quantitative assessment of changes in seasonal potential predictability for the twentieth century. *Climate Dynamics, 41*, 2697-2709. doi:10.1007/s00382-013-1874-x

Feudale, L., & Kucharski, F. (2013). A common mode of variability of African and Indian monsoon rainfall at decadal timescale. *Climate Dynamics*.

Fichefet, T., & Morales Maqueda, M. Á. (1997, June). Sensitivity of a global sea ice model to the treatment of ice thermodynamics and dynamics. *Journal of Geophysical Research, 1021*, 12609–12646. doi:10.1029/97JC00480

Forum, M. P. (1994). *MPI: A Message-Passing Interface Standard.* USA: University of Tennessee.

Fraedrich, K., Jansen, H., Kirk, E., Luksch, U., & Lunkeit, F. (2005, July 12). The Planet Simulator: Towards a user friendly model. *Meteorologische Zeitschrift, 14*, 299-304. doi:10.1127/0941-2948/2005/0043

Goosse, H., & Fichefet, T. (1999). Importance of ice-ocean interactions for the global ocean circulation: A model study. *Journal of Geophysical Research: Oceans, 104*, 23337–23355. doi:10.1029/1999JC900215

Gupta, A. S., Jourdain, N. C., Brown, J. N., & Monselesan, D. (2013, November). Climate Drift in the CMIP5 Models. *Journal of Climate, 26*, 8597–8615. doi:10.1175/JCLI-D-12-00521.1

Held, I. (2005, November). The Gap between Simulation and Understanding in Climate Modeling. *Bulletin of the American Meteorological Society, 86*, 1609-1614. doi:10.1175/bams-86-11-1609

Held, I. M., & Suarez, M. J. (1994, October). A Proposal for the Intercomparison of the Dynamical Cores of Atmospheric General Circulation Models. *Bulletin of the American Meteorological Society, 75*, 1825–1830. doi:10.1175/1520-0477(1994)075<1825:APFTIO>2.0.CO;2

Hersbach, H., Bell, B., Berrisford, P., Biavati, G., Horányi, A., Muñoz, . . . Thépaut, J.-N. (2019). ERA5 monthly averaged data on pressure levels from 1979 to present. Copernicus Climate Change Service (C3S) Climate Data Store (CDS). *ERA5 monthly averaged data on pressure levels from 1979 to present. Copernicus Climate Change Service (C3S) Climate Data Store (CDS)*. doi:10.24381/cds.6860a573

Hersbach, H., Bell, B., Berrisford, P., Biavati, G., Horányi, A., Muñoz, . . . Thépaut, J.-N. (2019). ERA5 monthly averaged data on single levels from 1979 to present. Copernicus Climate Change Service (C3S) Climate Data Store (CDS). *ERA5 monthly averaged data on single levels from 1979 to present. Copernicus Climate Change Service (C3S) Climate Data Store (CDS)*. doi:10.24381/cds.f17050d7

Huang, B., Thorne, P., Banzon, V., Boyer, T., Chepurin, G., Lawrimore, J., . . . Zhang, H.-M. (2017). NOAA Extended Reconstructed Sea Surface Temperature (ERSST), Version 5. *NOAA National Centers for Environmental Information*. doi:10.7289/V5T72FNM

ICTP - International Centre for Theoretical Physics. (n.d.). Retrieved 12 23, 2021, from Ictp.it: http://www.ictp.it/

IPCC. (2001). *Climate Change 2001: The Scientific Basis.*

Jackett, D. R., & Mcdougall, T. J. (1995). Minimal adjustment of hydrographic profiles to achieve static stability. *Journal of Atmospheric and Oceanic Technology, 12*, 381–389.

Kröger, J., & Kucharski, F. (2011). Sensitivity of ENSO characteristics to a new interactive flux correction scheme in a coupled GCM. *Climate Dynamics, 36*, 119–137. doi:10.1007/s00382-010-0759-5

Kucharski, F. (n.d.). *Speedy ver 41 Description.* Retrieved from http://users.ictp.it/~kucharsk/speedy_description/km_ver41_appendixA.pdf

Kucharski, F., Ikram, F., Molteni, F., Farneti, R., Kang, I.-S., No, H.-H., . . . Mogensen, K. (2015, June). Atlantic forcing of Pacific decadal variability. *Clim Dyn, 46*, 1-15. doi:10.1007/s00382-015-2705-z

Kucharski, F., Molteni, F., & Bracco, A. (2006). Decadal interactions between the western tropical Pacific and the North Atlantic Oscillation. *Climate Dynamics 26*, 79-91.

Kucharski, F., Molteni, F., King, M. P., Farneti, R., Kang, I.-S., & Feudale, L. (2013, January). On the Need of Intermediate Complexity General Circulation Models: A “SPEEDY” Example. *Bulletin of the American Meteorological Society, 94*, 25–30. doi:10.1175/BAMS-D-11-00238.1

Kucharski, F., Molteni, F., King, M. P., Farneti, R., Kang, I.-S., & Feudale, L. (2013). On the need of intermediate complexity general circulation models: a 'SPEEDY' example. *BAMS 94*, 25-30, DOI: 10.1175/BAMS-D-11-00238.1.

Kucharski, F., Zeng, N., & Kalnay, E. (2012). A further assessment of vegetation feedback on decadal Sahel rainfall variability. *Climate Dynamics*.

Kucharski, F., Zeng, N., & Kalnay, E. (2012). A further assessment of vegetation feedback on decadal Sahel rainfall variability. *Climate Dynamics*.

Lemaire, B. (2010). *doc_cfg_tools.pdf.* Retrieved from NEMO wiki: https://forge.ipsl.jussieu.fr/nemo/browser/utils/tools/GRIDGEN

Madec, G., & Delecluse, P. (n.d.). Ocean General Circulation Model Reference Manual. Retrieved from https://forge.ipsl.jussieu.fr/nemo/wiki/Documentation

Madec, G., Benshila, R., Bricaud, C., Coward, A., Dobricic, S., Furner, R., & Oddo, P. (2013, February). NEMO ocean engine. *Notes du Pôle de modélisation de l'Institut Pierre-Simon Laplace (IPSL) (v3.4, Number 27)*. doi:10.5281/zenodo.1464817

Masson-Delmotte, V., Zhai, P., Pirani, A., Connors, S., Péan, C., Berger, S., . . . Lonnoy, E. (2021). (T. W. J.B.R. Matthews, & B. Zhou, Eds.) *IPCC*.

Mcguffie, K., & Henderson-Sellers, A. (2014, March). *THE CLIMATE MODELLING PRIMER fourth edition.*

Mesinger, F., & Arakawa, A. (1976). Numerical methods used in atmospheric models.

Met Office. (2010 - 2015). *Cartopy: a cartographic python library with a matplotlib interface.* Exeter. Retrieved from http://scitools.org.uk/cartopy

Molteni, F. (2003). Atmospheric simulations using a GCM with simplified physical parametrizations. I. Model climatology and variability in multi-decadal experiments. *Climate Dynamics 20*, 175-191.

Molteni, F., King, M., Kucharski, F., & Straus, D. (2010, September 29). Planetary-scale variability in the northern winter and the impact of land–sea thermal contrast. *Climate Dynamics, 37*, 151-170. doi:10.1007/s00382-010-0906-z

NEMO ocean model. (n.d.). Retrieved from https://www.nemo-ocean.eu/

Petoukhov, V., Ganopolski, A., Brovkin, V., Claussen, M., Eliseev, A., Kubatzki, C., & Rahmstorf, S. (2000, January 3). CLIMBER-2: a climate system model of intermediate complexity. Part I: model description and performance for present climate. *Climate Dynamics, 16*, 1-17. doi:10.1007/pl00007919

Phillips, N. A. (1957, April). A COORDINATE SYSTEM HAVING SOME SPECIAL ADVANTAGES FOR NUMERICAL FORECASTING. *Journal of the Atmospheric Sciences, 14*, 184–185. doi:10.1175/1520-0469(1957)014<0184:ACSHSS>2.0.CO;2

Platov, G., Krupchatnikov, V., Martynova, Y., Borovko, I., & Golubeva, E. (2017, November). A new earth's climate system model of intermediate complexity, PlaSim-ICMMG-1.0: description and performance. *IOP Conference Series: Earth and Environmental Science, 96*, 012005. doi:10.1088/1755-1315/96/1/012005

Robert, A. J. (1966). The integration of a low order spectral form of the primitive meteorological equations. *Journal of the Meteorological Society of Japan. Ser. II, 44*, 237–245.

Schulzweida, U. (2020). CDO User Guide. doi:10.5281/ZENODO.5614769

Sluka, T. C., Penny, S. G., Kalnay, E., & Miyoshi, T. (2016, January). Assimilating atmospheric observations into the ocean using strongly coupled ensemble data assimilation. *Geophysical Research Letters, 43*, 752–759. doi:10.1002/2015gl067238

Stouffer, R. J., Hegerl, G., & Tett, S. (2000, February). A Comparison of Surface Air Temperature Variability in Three 1000-Yr Coupled Ocean–Atmosphere Model Integrations. *Journal of Climate, 13*, 513–537. doi:10.1175/1520-0442(2000)013<0513:ACOSAT>2.0.CO;2

Timmermann, R., Goosse, H., Madec, G., Fichefet, T., Ethe, C., & Duliere, V. (2005). On the representation of high latitude processes in the ORCA-LIM global coupled sea ice–ocean model. *Ocean Modelling, 8*, 175–201.

Timmermann, R., Goosse, H., Madec, G., Fichefet, T., Ethé, C., & Dulière, V. (2005, December). On the representation of high latitude processes in the ORCA-LIM global coupled sea ice-ocean model. *Ocean Modelling, 8*, 175–201. doi:10.1016/j.ocemod.2003.12.009

Valcke, S. (2013, March). The OASIS3 coupler: a European climate modelling community software. *Geoscientific Model Development, 6*, 373–388. doi:10.5194/gmd-6-373-2013

Van Rossum, G., & Drake, F. (2009). Python 3 Reference Manual. *Python 3 Reference Manual*. Scotts, Valley, CA: CreateSpace.

Walsh, J. E., Chapman, W. L., & Fetterer, F. (2019). Gridded Monthly Sea Ice Extent and Concentration, 1850 Onward, Version 2. *Gridded Monthly Sea Ice Extent and Concentration, 1850 Onward, Version 2*. NSIDC. doi:10.7265/JJ4S-TQ79

Wild, M. (2020, August). The global energy balance as represented in CMIP6 climate models. *Climate Dynamics, 55*, 553–577. doi:10.1007/s00382-020-05282-7

APPENDIX: SPEEDY-NEMO Output Files

SPEEDY-NEMO output files are listed below. For each file output variable name, description and units are shown.

SPEEDY files are in GRIB format while NEMO files are in NetCDF format. A NEMO multiprocessor run generates one output file for each domain in which oceans have been divided. The single domain files can be reassembled as described in paragraph 5.1. Files are numbered starting from 0. See Figure 8 for the numeration of an 8x2 run.

attm<exp>.ctl (SPEEDY) (<exp>, the experiment number identifies the run)

gh	geopotential height	[m]
temp	abs. temperature	[°K]
u	zonal (u) wind	[m/s]
v	meridional (v) wind	[m/s]
q	specific humidity	[g/Kg]
rh	relative humidity	[%]
omega	pressure vertical velocity	[Pa/s]
psi	streamfunction	[10^6 m^2/s]
chi	velocity potential	[10^6 m^2/s]
sp	surface pressure	[hPa]
mslp	mean-sea-level pressure	[hPa]
st	surface temperature	[°K]
skint	skin temperature	[°K]
swav	soil wetness availability	[%]
alb	surface albedo	[%]
sice	sea ice fraction	[%]
u0	near-surface u-wind	[m/s]
v0	near-surface v-wind	[m/s]
temp0	near-surface air temperature	[°K]
rh0	near-surface relative humidity	[%]

clc	cloud cover (deep clouds)	[%]
clstr	cloud cover (strat. clouds)	[%]
cltop	pressure at cloud top	[hPa]
iptop	highest precipitation level index	[]
lst	land-surface temp.	[°K]
sst	sea-surface temp.	[°K]
sstom	ocean model sea-surface temp.	[°K]
siceom	ocean model sea ice fraction	[%]
ssta	SST anomaly w.r.t. obs. clim.	[°K]
precls	large-scale precipitation	[mm/day]
precnv	convective precipitation	[mm/day]
evap	evaporation	[mm/day]
ustr	u-stress (dw.)	[N/m^2]
vstr	v-stress (dw.)	[N/m^2]
tsr	top shortwave rad. (dw.)	[W/m^2]
olr	outgoing longwave rad. (uw.)	[W/m^2]
ssr	surface shortwave rad. (dw.)	[W/m^2]
slr	surface longwave rad. (uw.)	[W/m^2]
shf	sensible heat flux (uw.)	[W/m^2]
lshf	heat flux into land sfc (dw.)	[W/m^2]
sshf	heat flux into sea sfc (dw.)	[W/m^2]

atva<exp>.ctl (SPEEDY)

vargh:	variance of geop. height	[m^2]"
vart:	variance of temperature	[degK^2]"
varu:	variance of u-wind	[J/Kg]"
varv:	variance of v-wind	[J/Kg]"
covuv:	u'v' covariance (trans.)	[J/Kg]"
covvt:	v'T' covariance (trans.)	[degK m/s]"

atdf<exp>.ctl (SPEEDY)

dtlsc:	dT/dt by large-scale cond	[°K/day]"
dtcnv:	dT/dt by convection	[°K/day]"
dtrsw:	dT/dt by shortwave rad	[°K/day]"
dtrlw:	dT/dt by longwave rad	[°K/day]"
dtpbl:	dT/dt by PBL processes	[°K/day]"

ORCA2_1m_<startdate>_<enddate>_icemod.nc (NEMO)

isnowthi:	"Snow thickness"	"m"
iicethic:	"Ice thickness"	"m"
iiceprod:	"Ice produced"	"m/kt"
ileadfra:	"Ice concentration"	"%"
iicetemp:	"Ice temperature"	"C"
ioceflxb:	"Oceanic flux at the ice base"	"w/m^2"
iicevelu:	"Ice velocity u"	"m/s"
iicevelv:	"Ice velocity v"	"m/s"
isursenf:	"Sensible Heat Flux"	"w/m^2"
isurlowf:	"Infra-red Heat Flux"	"w/m^2"
iocetflx:	"Total flux at ocean surface"	"w/m^2"
iocesflx:	"Solar flux at ocean surface"	"w/m^2"
iocwnsfl:	"Non-solar flux at ocean surface"	"w/m^2"
iocesafl:	"Salt flux at ocean surface"	"kg/m^2/kt"
iocestru:	"Wind stress u"	"Pa"
iocestrv:	"Wind stress v"	"Pa"
iicesflx:	"Solar flux at ice/ocean surface"	"w/m^2"
iicenflx:	"Non-solar flux at ice/ocean surface"	"w/m^2"
isnowpre:	"Snow precipitation"	"kg/day"

ORCA2_1m_<startdate>_<enddate>_grid_V.nc (NEMO)

vomecrty:	"Meridional Current"	"m/s"
vomeeivv:	"Meridional EIV Current"	"m/s"
sometauy:	"Wind Stress along j-axis"	"N/m^2"

ORCA2_1m_<startdate>_<enddate>_grid_U.nc (NEMO)

vozocrtx:	"Zonal Current"	"m/s"
vozoeivu:	"Zonal EIV Current"	"m/s"
sozotaux:	"Wind Stress along i-axis"	"N/m^2"

ORCA2_1m_<startdate>_<enddate>_grid_W.nc (NEMO)

vovecrtz:	"Vertical Velocity"	"m/s"
voveeivw:	"Vertical EIV Velocity"	"m/s"
votkeavt:	"Vertical Eddy Diffusivity"	"m^2/s"
votkeevd:	"Enhanced Vertical Diffusivity"	"m^2/s"
votkeavm:	"Vertical Eddy Viscosity"	"m^2/s"
votkeevm:	"Enhanced Vertical Viscosity"	"m^2/s"
voddmavs:	"Salt Vertical Eddy Diffusivity"	"m^2/s"
soleahtw:	"lateral eddy diffusivity"	"m^2/s"
soleaeiw:	"eddy induced vel. coeff. at w-point"	"m^2/s"

"ORCA2_1m_<startdate>_<enddate>_grid_T.nc (NEMO)

votemper:	"Temperature"	"C"
vosaline:	"Salinity"	"PSU"
sosstsst:	"Sea Surface temperature"	"C"
sosaline:	"Sea Surface Salinity"	"PSU"
sossheig:	"Sea Surface Height"	"m"
iowaflup:	"Ice=>ocean net freshwater"	"kg/m^2/s"
sowaflep:	"atmos=>ocean net freshwater"	"kg/m^2/s"
sowaflup:	"Net Upward Water Flux"	"Kg/m^2/s"
sorunoff:	"Runoffs"	"Kg/m^2/s"
sowaflcd:	"concentration/dilution water flux"	"kg/m^2/s"
sosalflx:	"Surface Salt Flux"	"Kg/m^2/s"
sohefldo:	"Net Downward Heat Flux"	"W/m^2"

soshfldo:	"Shortwave Radiation"	"W/m^2"
somxl010:	"Mixed Layer Depth 0.01"	"m"
somixhgt:	"Turbocline Depth"	"m"
soicecov:	"Ice Cover"	"[0,1]"
sobowlin:	"Bowl Index"	"W-point"
soicetem:	"Ice Surface Temperature"	"K"
soicealb:	"Ice Albedo"	"[0,1]"